Examples of Beam Diagnostic Techniques

- Trajectories and Orbit Distortions
- Tune Measurements
- Amplitude Function Measurements
  - Ex's: tune shift method; AC dipole method
- Chromaticity Measurements
- Dispersion Measurements
- Emittance Measurements
  - emittance vs. momentum spread; tomography
- Coupling Measurements
- Phase Space Measurements
  - turn-by-turn, at 2 BPMs
- Nonlinear Tune-shift, Dynamic Aperture, & Diffusion

Beam Current Instruments

- Faraday cup

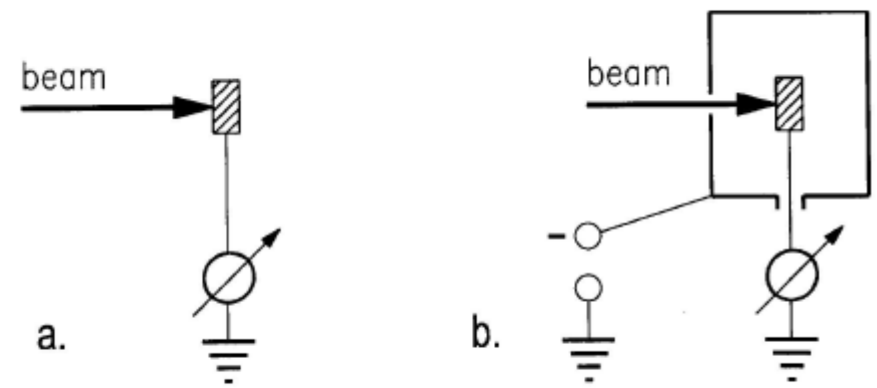

Fig. 15 a) Simple collector; b) Proper Faraday Cup.

Source: Koziol, *Beam Diagnostics for Accelerators,* CERN 1998

- Current Transformer

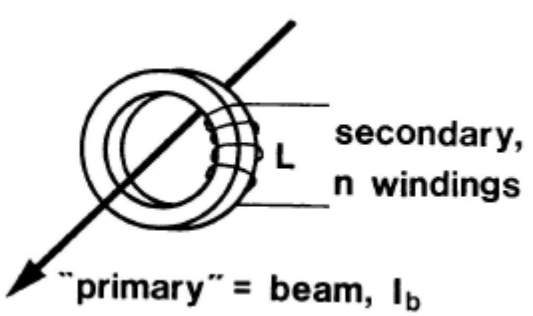

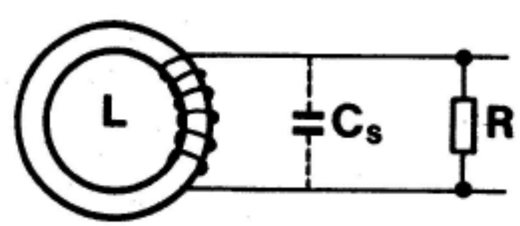

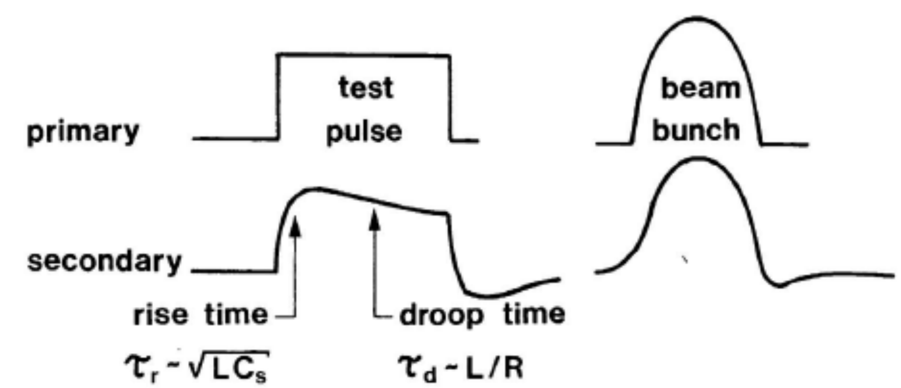

Wall Current Monitor

- Image charges
  - Moving beams make images on the wall of the pipe.
  - Length of image depends on β
  - Image current goes as beam current

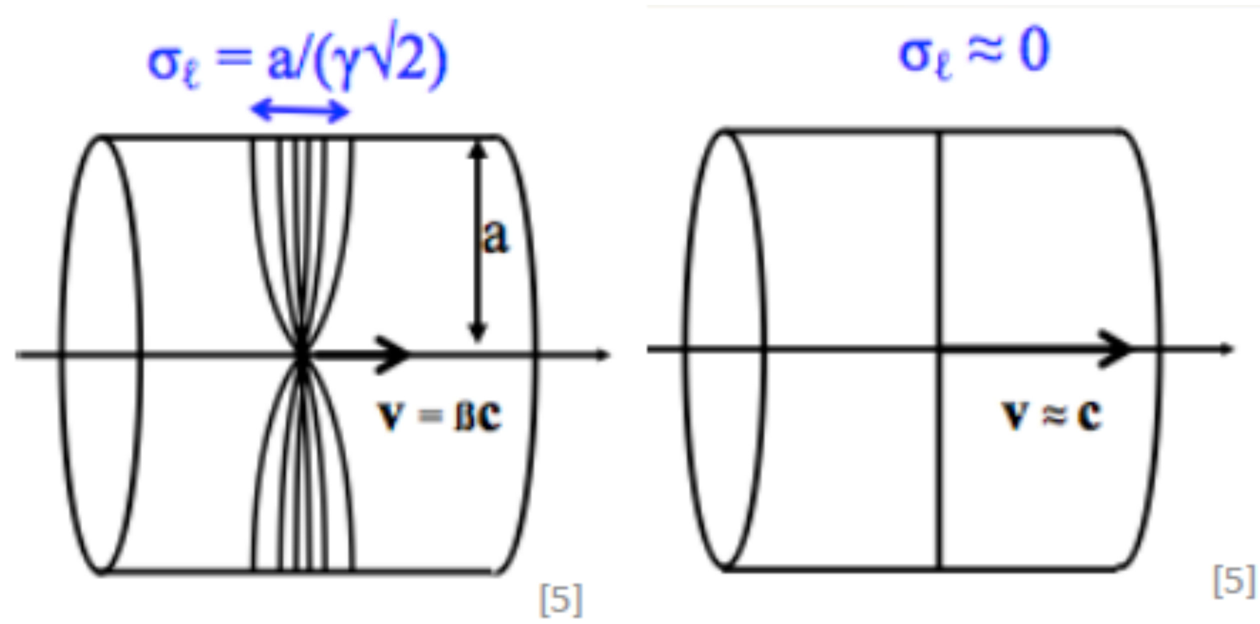

Moving charge

Fast moving charge

Source: Denard, J.C. *CERN Accelerator School on Beam Diagnostics, 2008*

- Wall Current Monitor
  - Replace pipe with R
  - Measure I across R
  - Box needed to keep pipe grounded
  - Use ferrite to force I across R

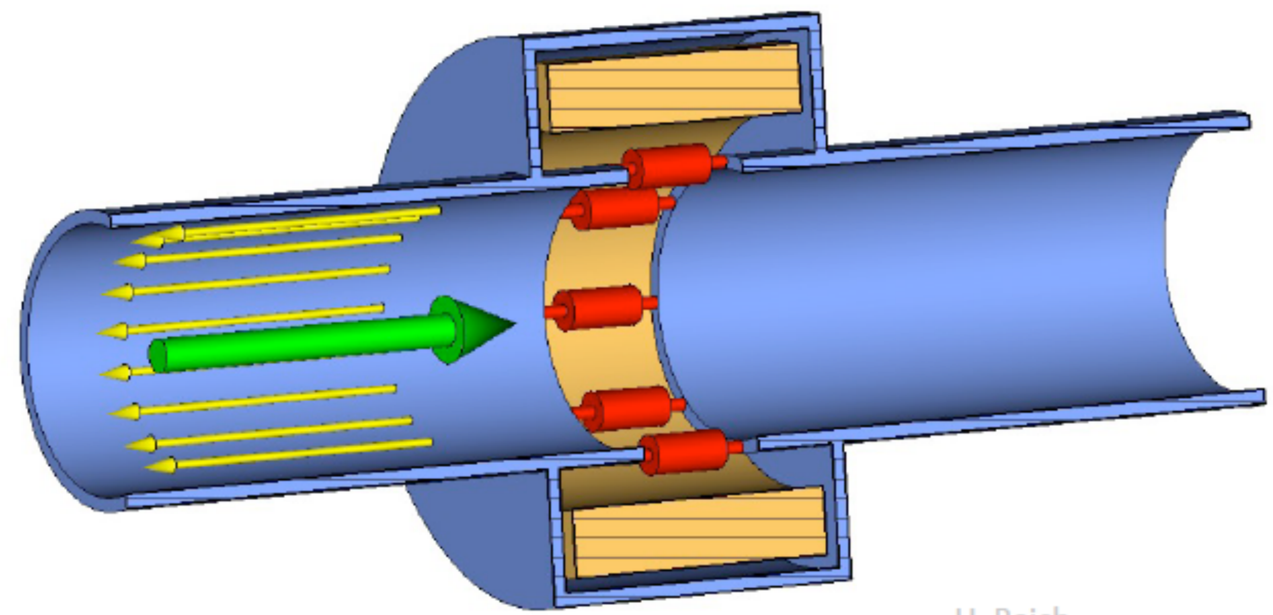

Source: Raich U, reprinted by Blokland, W. in *Beam Current Monitors,* USPAS 2009

D. Alt, Winter 2016 USPAS

Beam Loss Monitor Types

- Ionization Chambers
  - Filled with inert gas
  - Potential Difference
  - Radiation ionizes gas, generates current

Source: FNAL

Visualisation of ion chamber operation

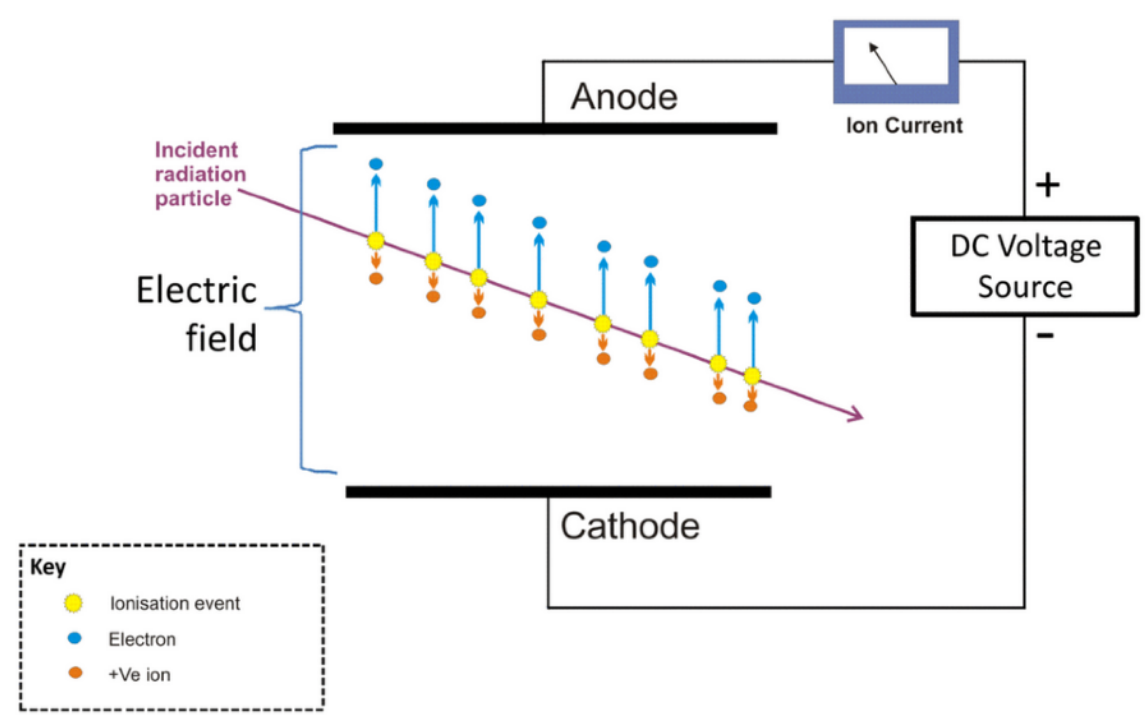

Source: *Knoll, Glenn F (1999). Radiation detection and measurement (3rd ed.).*

D. Alt, Winter 2016 USPAS

Beam Loss Monitor Types

- Scintillation Detector
  - Radiation strikes scintillator, generates photon
  - Detected by photomultiplier tube

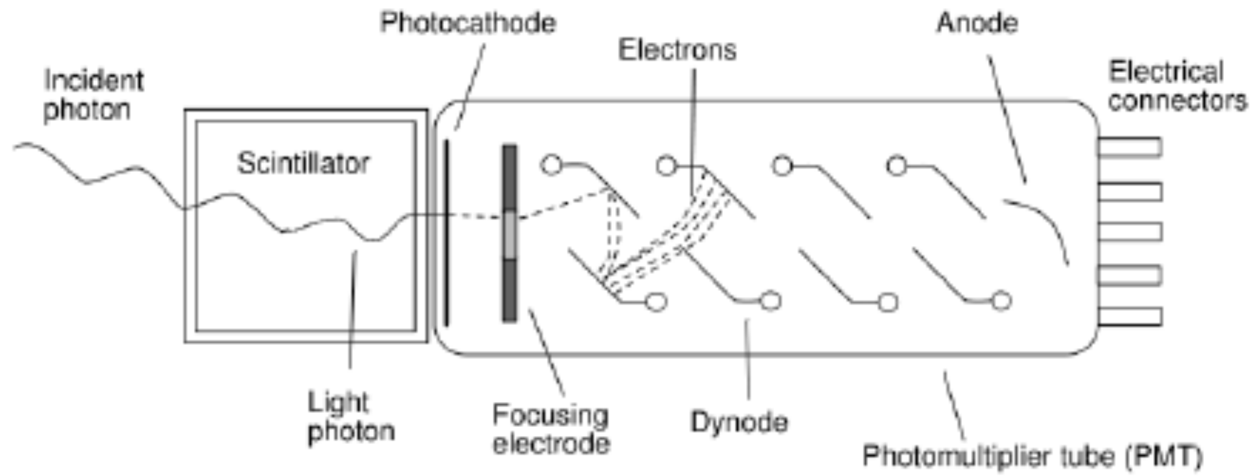

Source: Zhokov, A. *Beam Loss Monitors,* USPAS 2009

- Cerenkov Detector
  - Uses Cerenkov effect
  - Instantaneous
  - Threshold = background filter
  - Lower sensitivity than scintillator

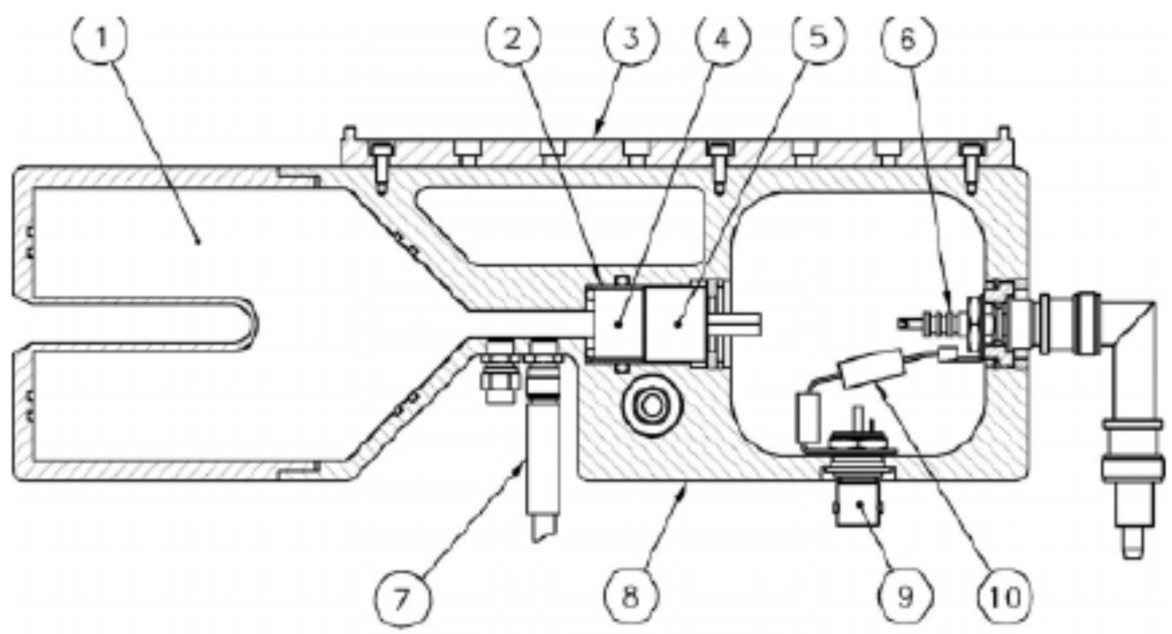

Source: W. Berg, LCLS BLM, TUP043 LINAC08

Orbit / Position Measurement

- Beam Position Monitor (various styles)

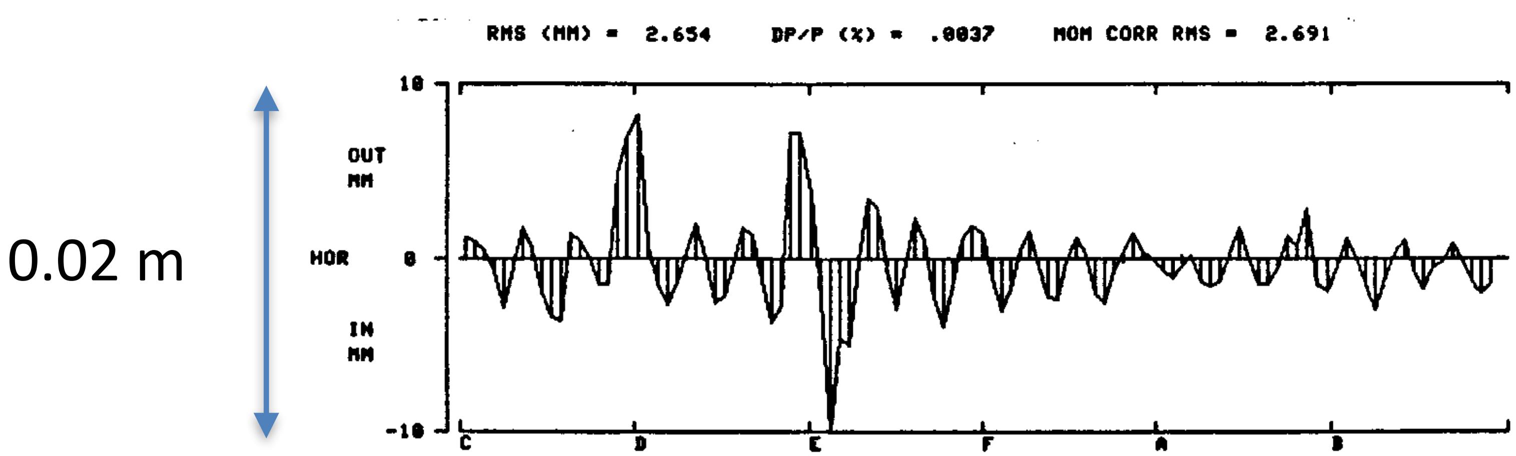

Figure 3.8: Experimental data of the closed orbit.

6283 m

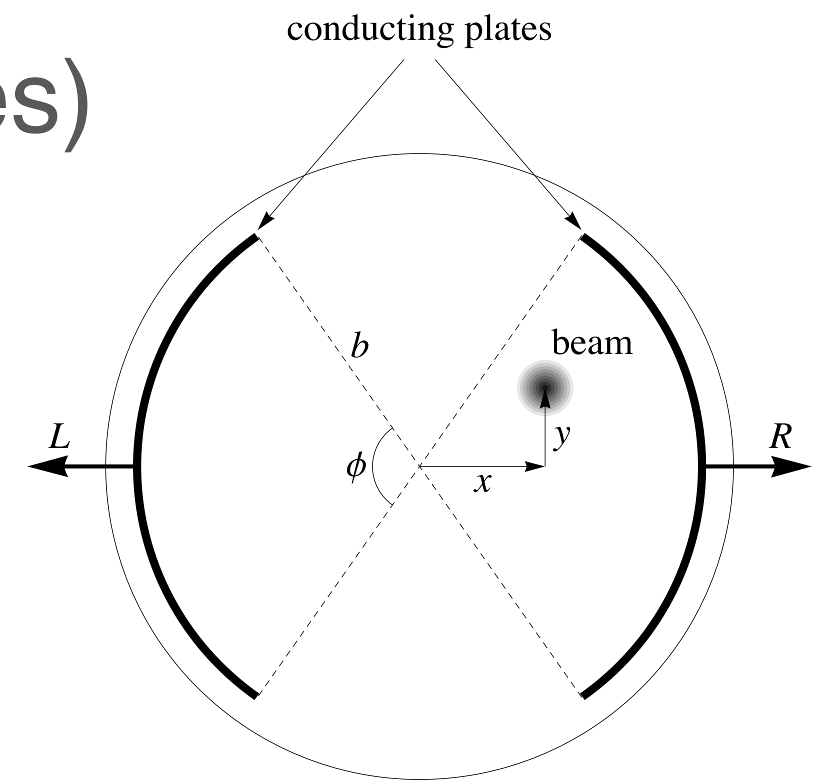

- Single pass — determine trajectory of centroid
- Some average over many passes
  - e.g., to determine the closed orbit

BPM Design Choices

- Button pick-ups

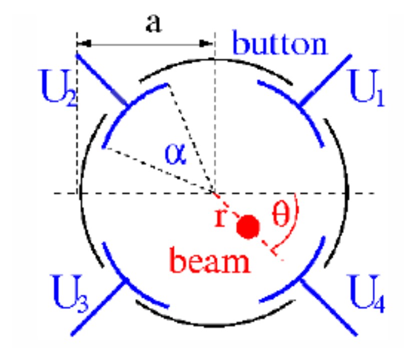

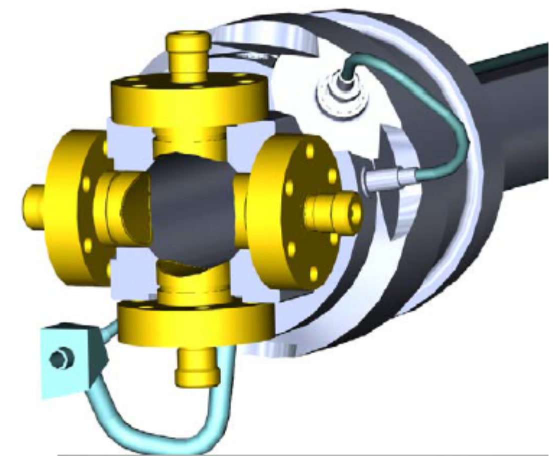

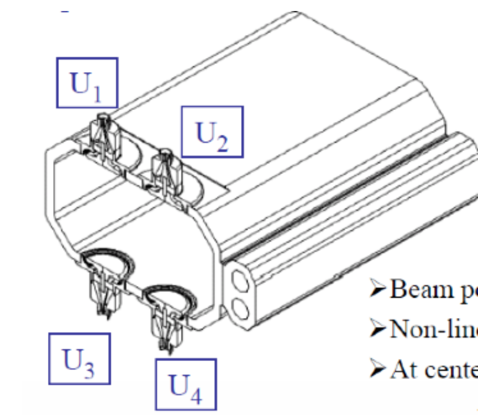

- Cavity

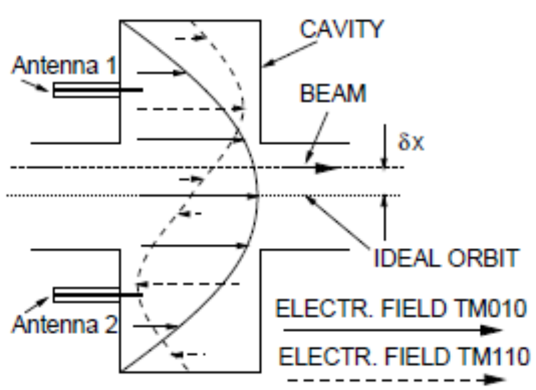

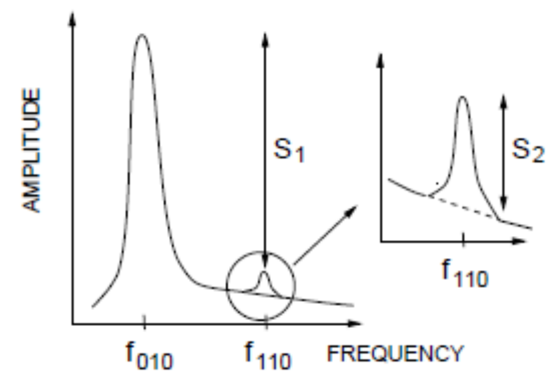

Source: Lorenz, R. *Cavity Beam Position Monitors,* BIW98

- Stripline

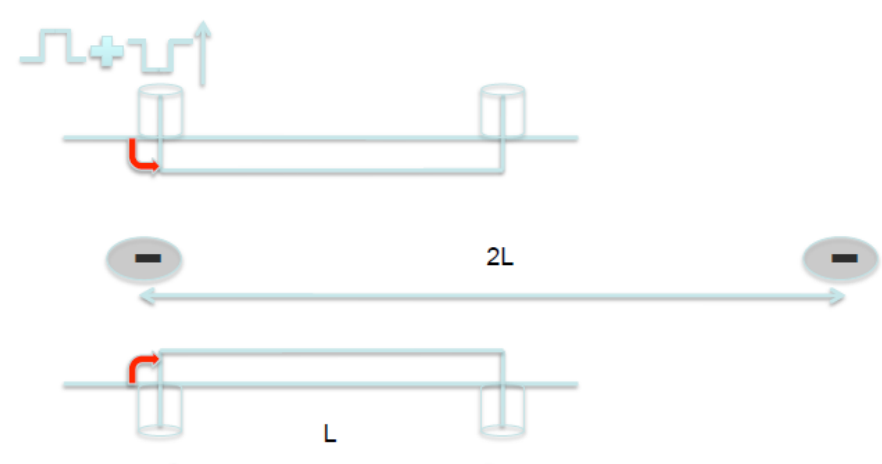

Source: Byrd, J. 2009

Data Taking

- Take position data
- Make a change (kicker magnet, steering magnet, etc.)
- Re-take data
- Subtract and plot the difference

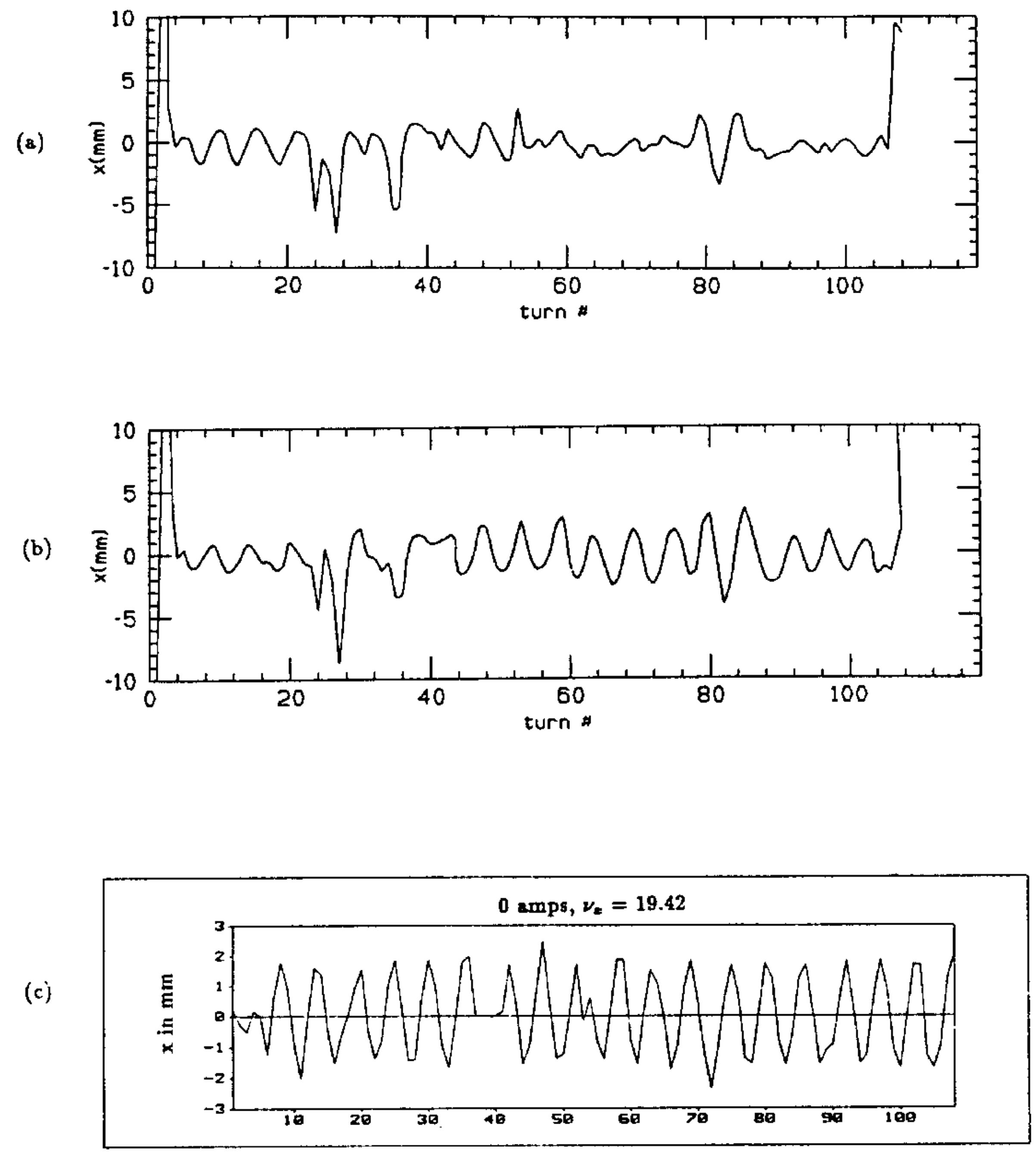

the induced betatron oscillation

Tune Measurements

- measure betatron tune using *single* BPM signal
  - use kicker magnet to induce betatron oscillation
  - from FFT analysis, determine the frequency

Data: (a)

Frequency Spectrum: (b)

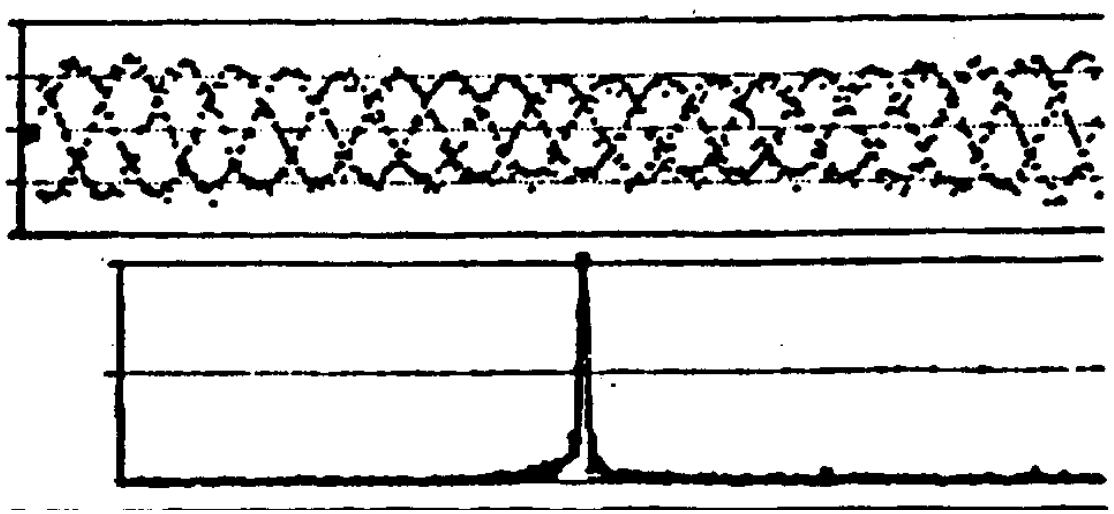

- tune does not depend upon position
  - *prove* !

Amplitude Function Measurements

- Tune shift measurement

$$\Delta\nu \approx \frac{1}{4\pi}\beta_0 q$$

- orbit/trajectory response

$$x(s) = \Delta\theta\sqrt{\beta_0\beta(s)}\,\sin[\psi(s)-\psi_0]$$

change in downstream trajectory

$$\Delta x(s) = \frac{\Delta\theta\sqrt{\beta_0\beta(s)}}{2\sin\pi\nu}\,\cos\left[|\psi(s)-\psi_0|-\pi\nu\right]$$

change in closed orbit

AC Dipole Measurements

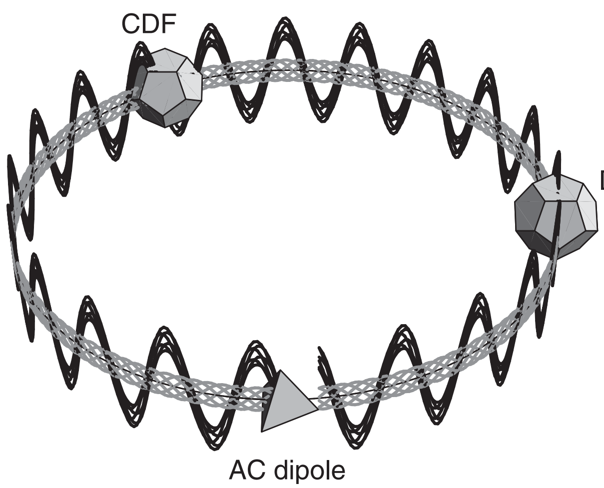

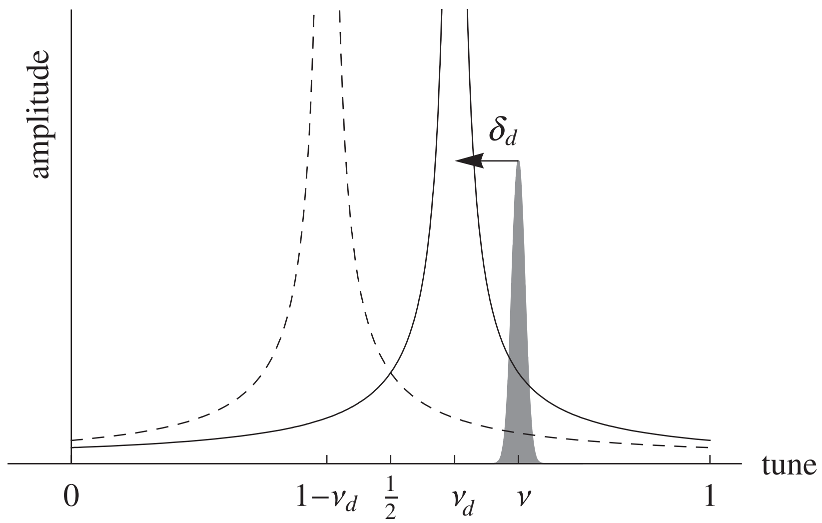

PHYSICAL REVIEW SPECIAL TOPICS - ACCELERATORS AND BEAMS **11**, 084002 (2008)

Parametrization of the driven betatron oscillation

R. Miyamoto and S. E. Kopp
Department of Physics, University of Texas at Austin, Austin, Texas 78712, USA

A. Jansson and M. J. Syphers
Fermi National Accelerator Laboratory, Batavia, Illinois 60510, USA
(Received 18 September 2007; published 27 August 2008)

An AC dipole is a magnet which produces a sinusoidally oscillating dipole field and excites coherent transverse beam oscillations in a synchrotron. By observing this driven coherent oscillation, the linear optical parameters can be directly measured at locations of the beam position monitors. The driven oscillations induced by an AC dipole will generate a phase space ellipse which differs from that of free oscillations. If not properly accounted for, this difference can lead to misinterpretations of the actual optical parameters, for instance, 6% or more in the cases of the Tevatron, RHIC, or LHC. This paper shows that the effect of an AC dipole on the observed linear optics is identical to that of a thin lens quadrupole. By introducing a new amplitude function to describe this new phase space ellipse, the motion produced by an AC dipole becomes easier to interpret. The introduction of this new amplitude function also helps measurements of the normal Courant-Snyder parameters based on beam position data taken under the influence of an AC dipole. This new parametrization of driven oscillations is presented and is used to interpret data taken in the FNAL Tevatron using an AC dipole.

PARAMETRIZATION OF THE DRIVEN BETATRON ...

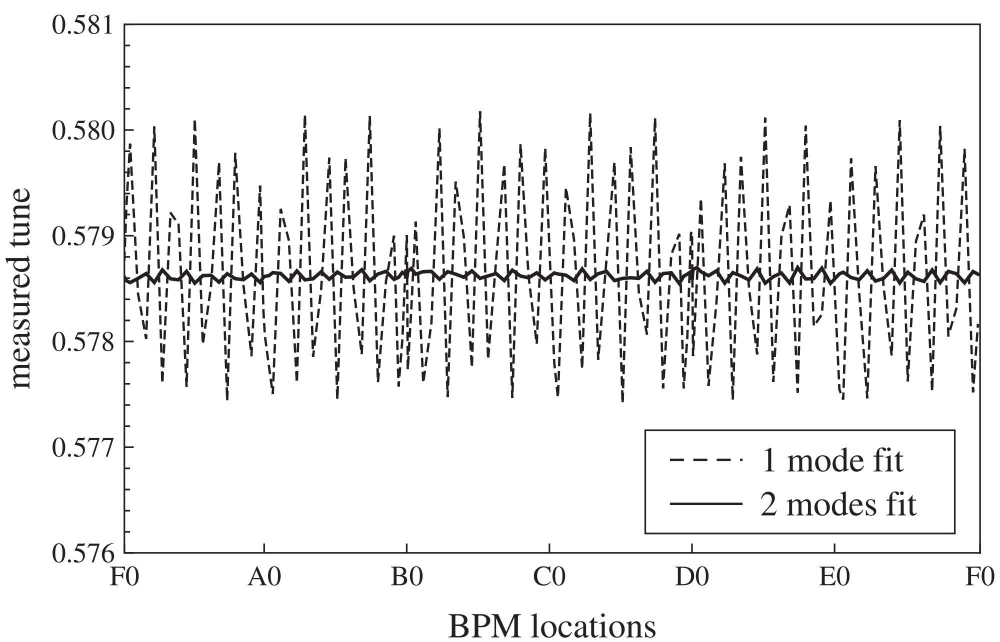

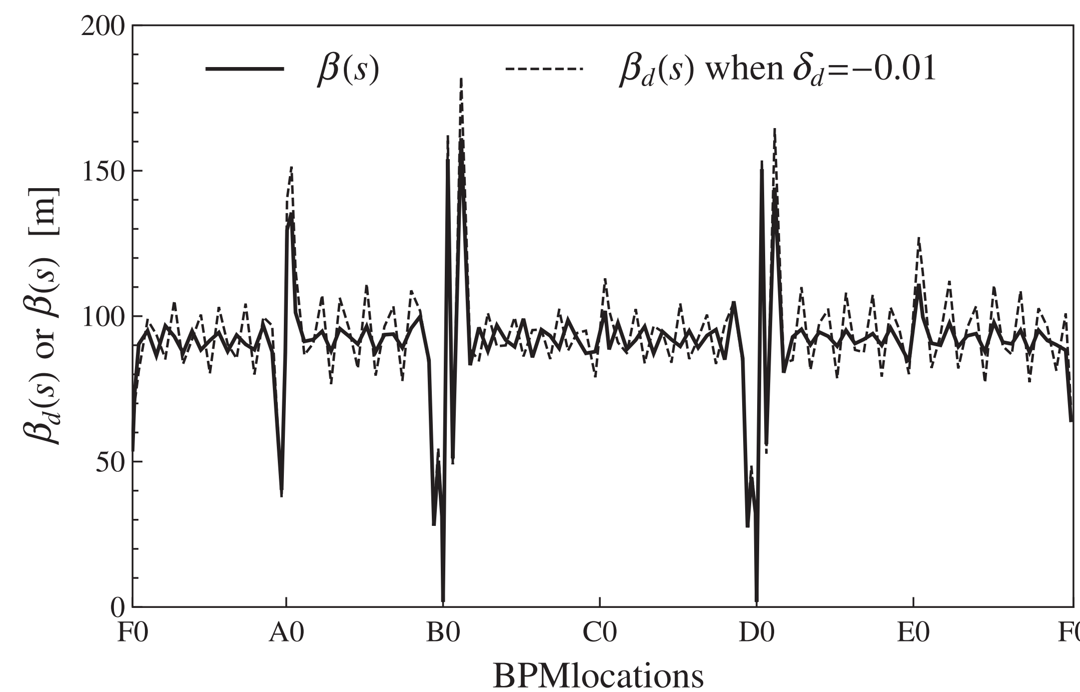

FIG. 4. The amplitude functions of free and driven oscillations, $\beta(s)$ (solid) and $\beta_d(s)$ when $\delta_d = -0.01$ (dashed), in the Tevatron. As expected, $\beta_d(s)$ shows beating with 10%–15% peak height relative to $\beta(s)$. From multiple data sets of driven oscillations, the amplitude function of free oscillations, $\beta(s)$, can be extrapolated.

Chromaticity Measurements

- vary the momentum of the beam in a synchrotron by varying the RF frequency; then, kick the beam and measure the tune

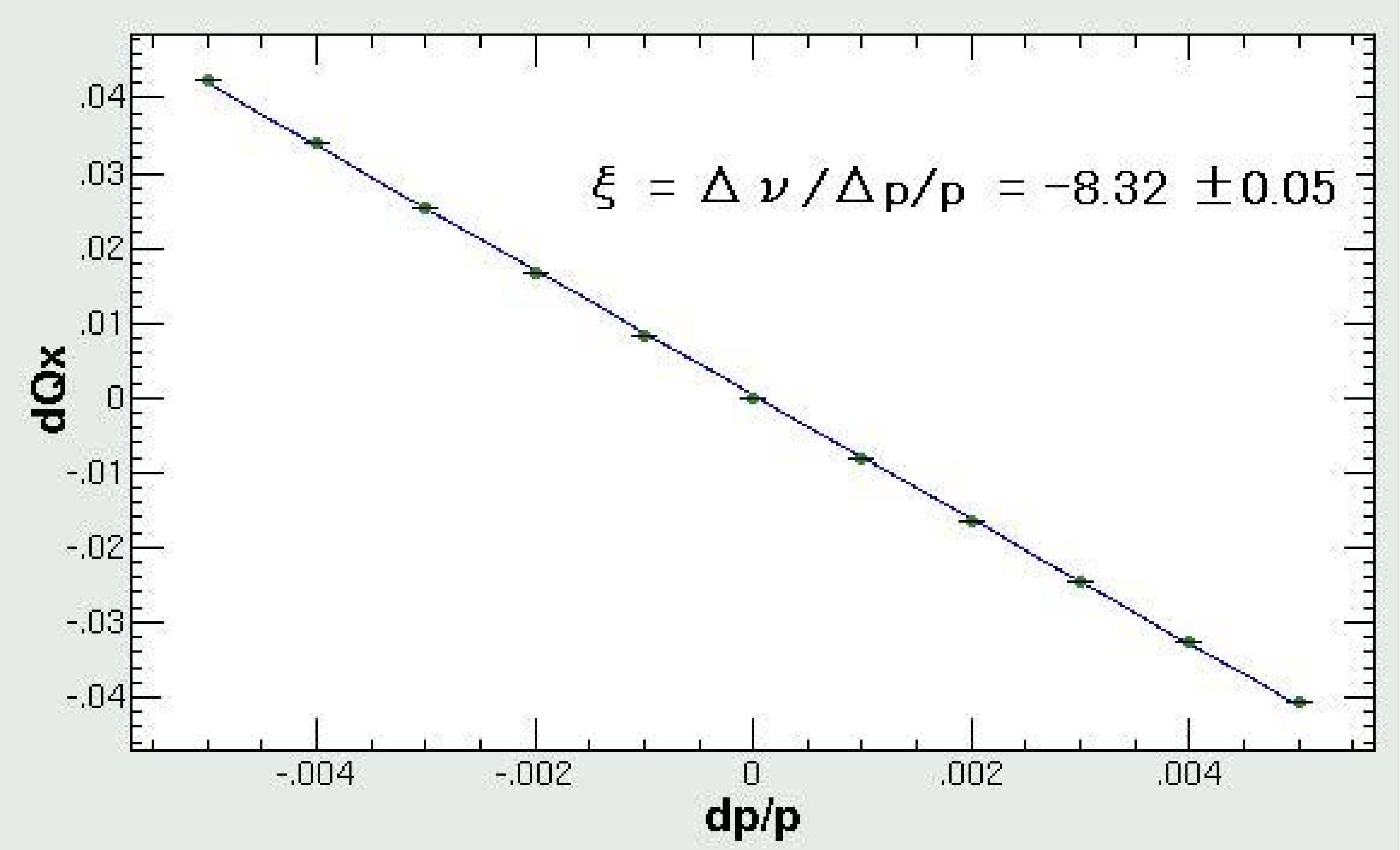

$$\xi \equiv \frac{\Delta\nu}{\Delta p/p}$$

J-PARC 3 GEV RAPID CYCLING SYNCHROTRON

EPAC2006

Dispersion Measurements

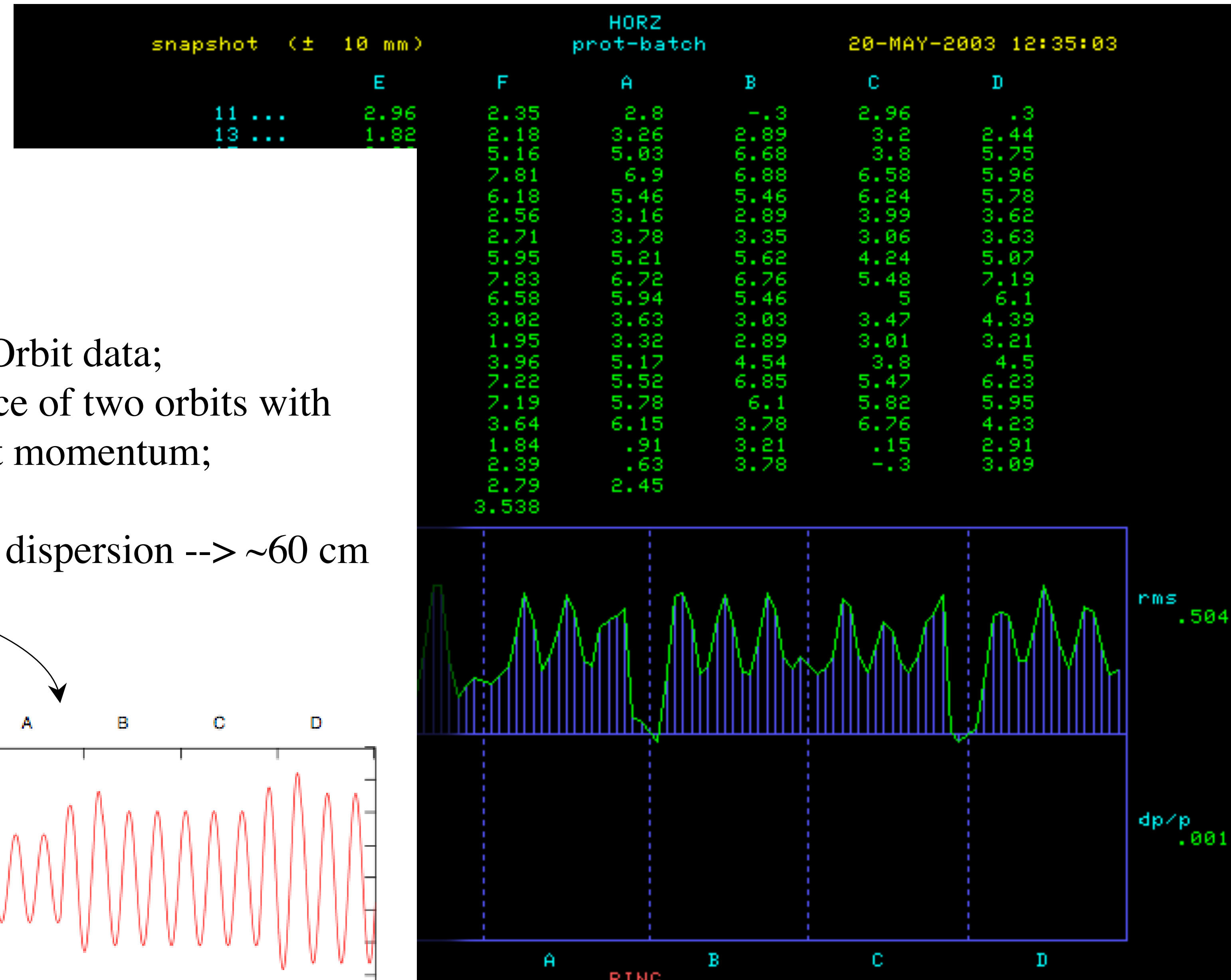

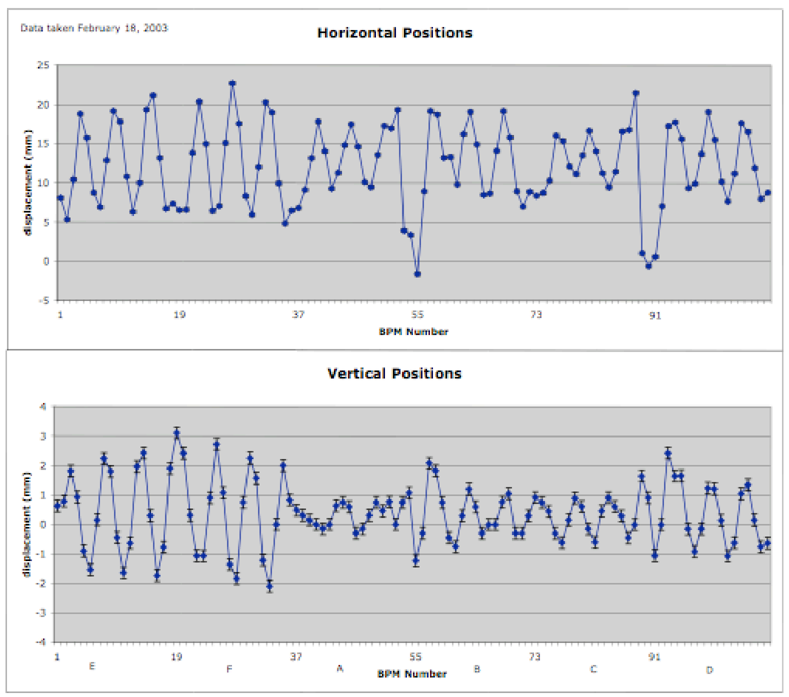

Closed Orbit data;
difference of two orbits with different momentum;
Note:
vertical dispersion --> ~60 cm

Simple calculation of dispersion wave generated by Tevatron skew quad circuits + large a_1 in main dipole magnets

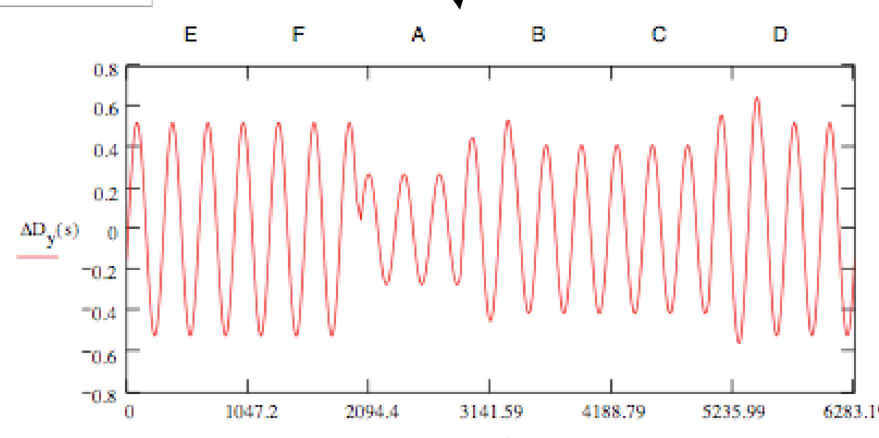

Measurement of Global Coupling

Coupled harmonic oscillator has two eigenvalues

$q := 2 \qquad \omega_2 := 15$

$\omega_1 := 10, 10.01 .. 20$

$$\omega_m(\omega_1) := \sqrt{\frac{\omega_1^2 + \omega_2^2 - \sqrt{\left(\omega_2^2 - \omega_1^2\right)^2 + 4 \cdot q^4}}{2}}$$

$$\omega_p(\omega_1) := \sqrt{\frac{\omega_1^2 + \omega_2^2 + \sqrt{\left(\omega_2^2 - \omega_1^2\right)^2 + 4 \cdot q^4}}{2}}$$

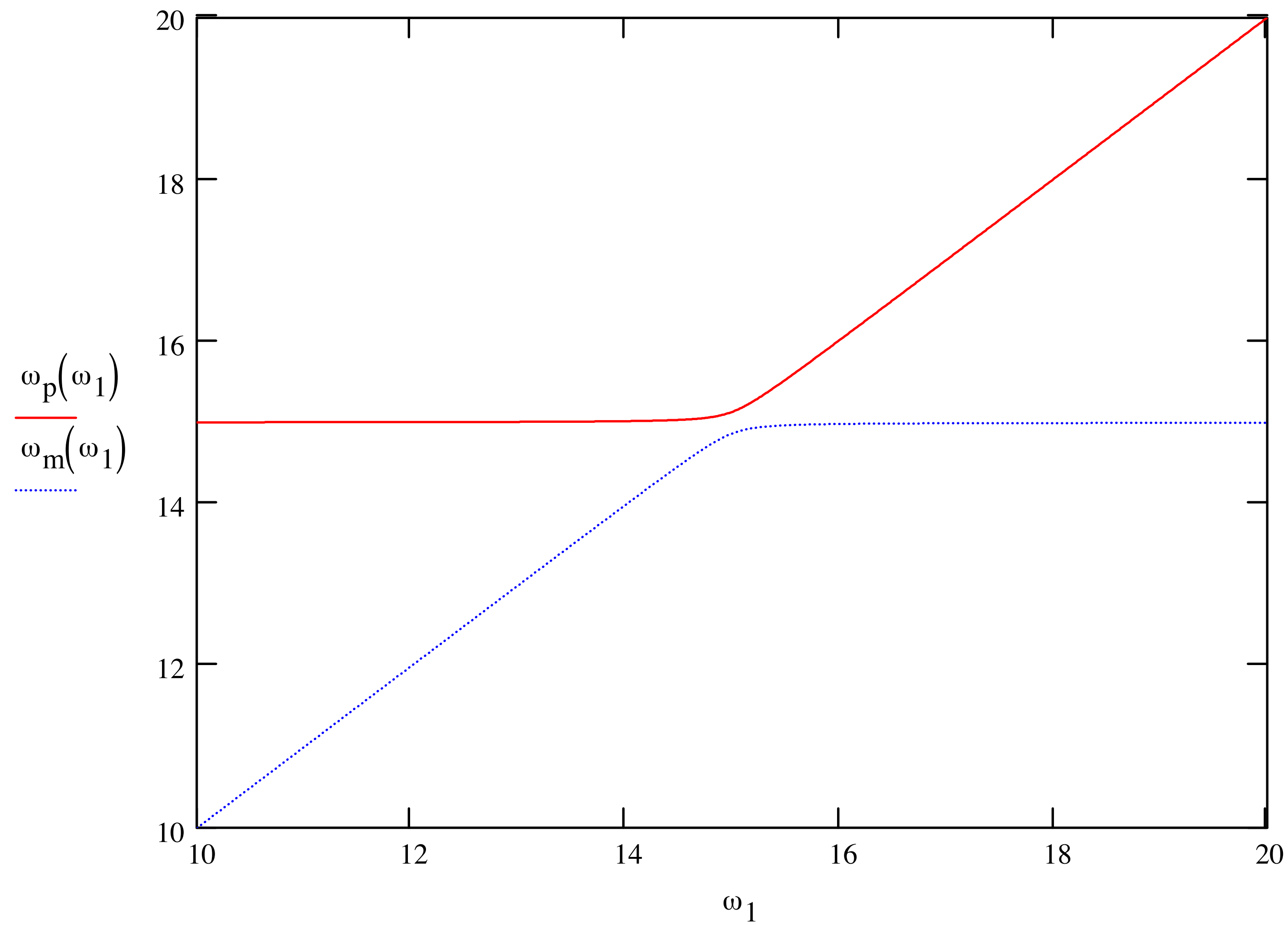

Measurement of Global Coupling

Coupled harmonic oscillator has two eigenvalues

When the natural frequencies in the horizontal and vertical tunes are far apart, they behave rather independently. However, they can never be made identical. So, by varying the quadrupoles in a ring to vary the tunes, the minimum separation observed is a measure of the amount of coupling, in a global sense, between the two planes

Adjust horizontal tune, say, and measure both horizontal and vertical tunes w/ FFT of BPM data. For a single rotated quadrupole,

$$\delta\nu_{min} = \frac{|\phi|}{\pi}\frac{\sqrt{\beta_x\beta_y}}{F}$$

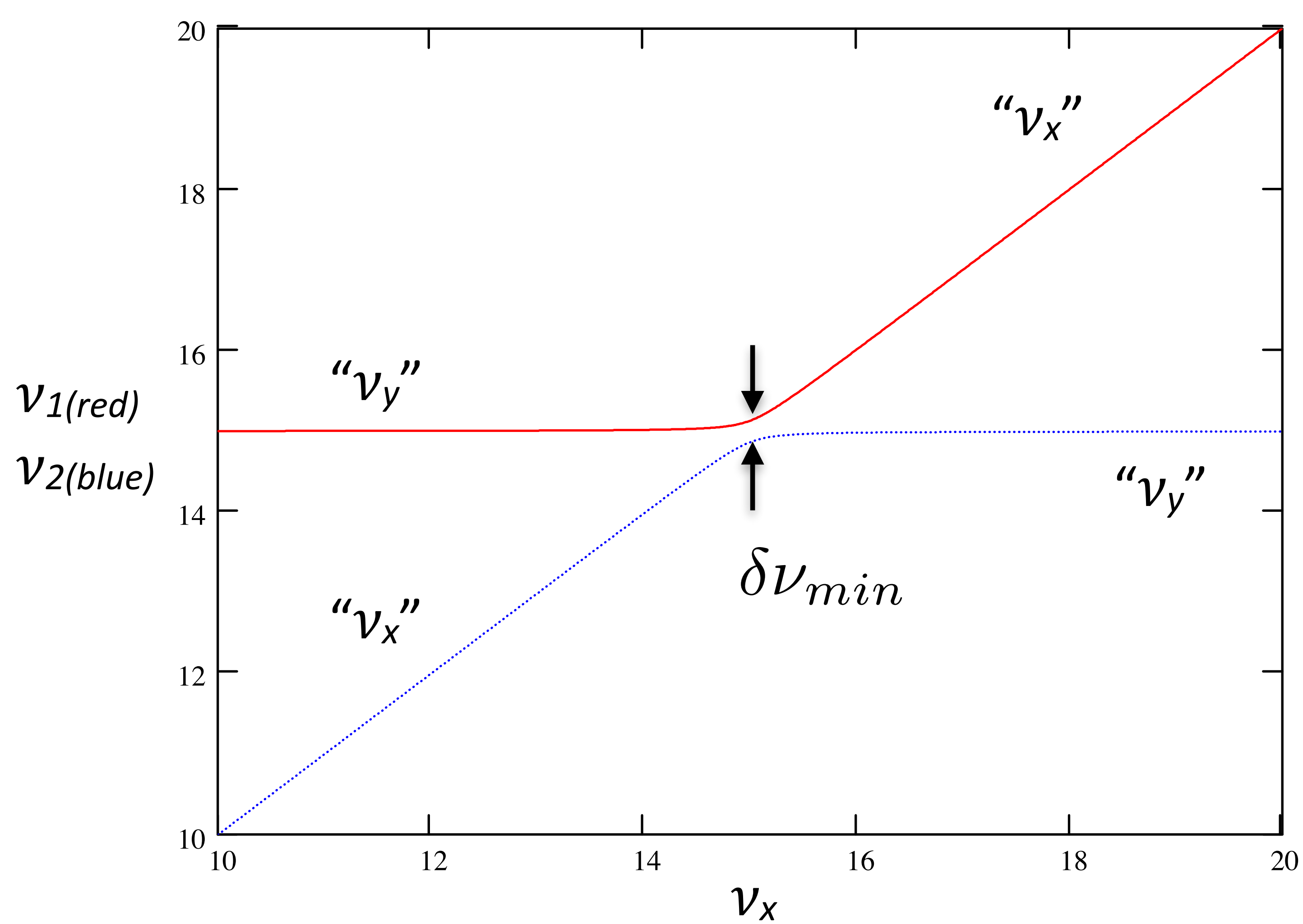

Coupling Measurements

- Global Coupling

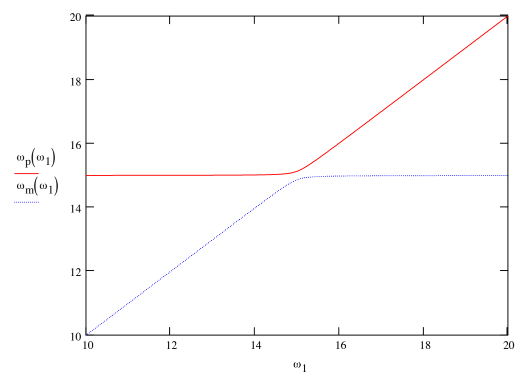

- Local Coupling

LOCAL vs. GLOBAL Coupling

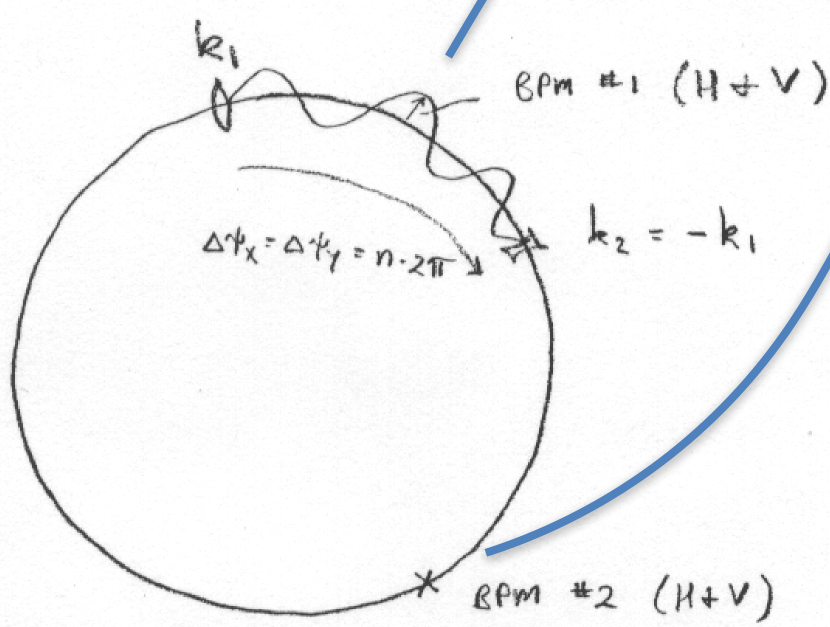

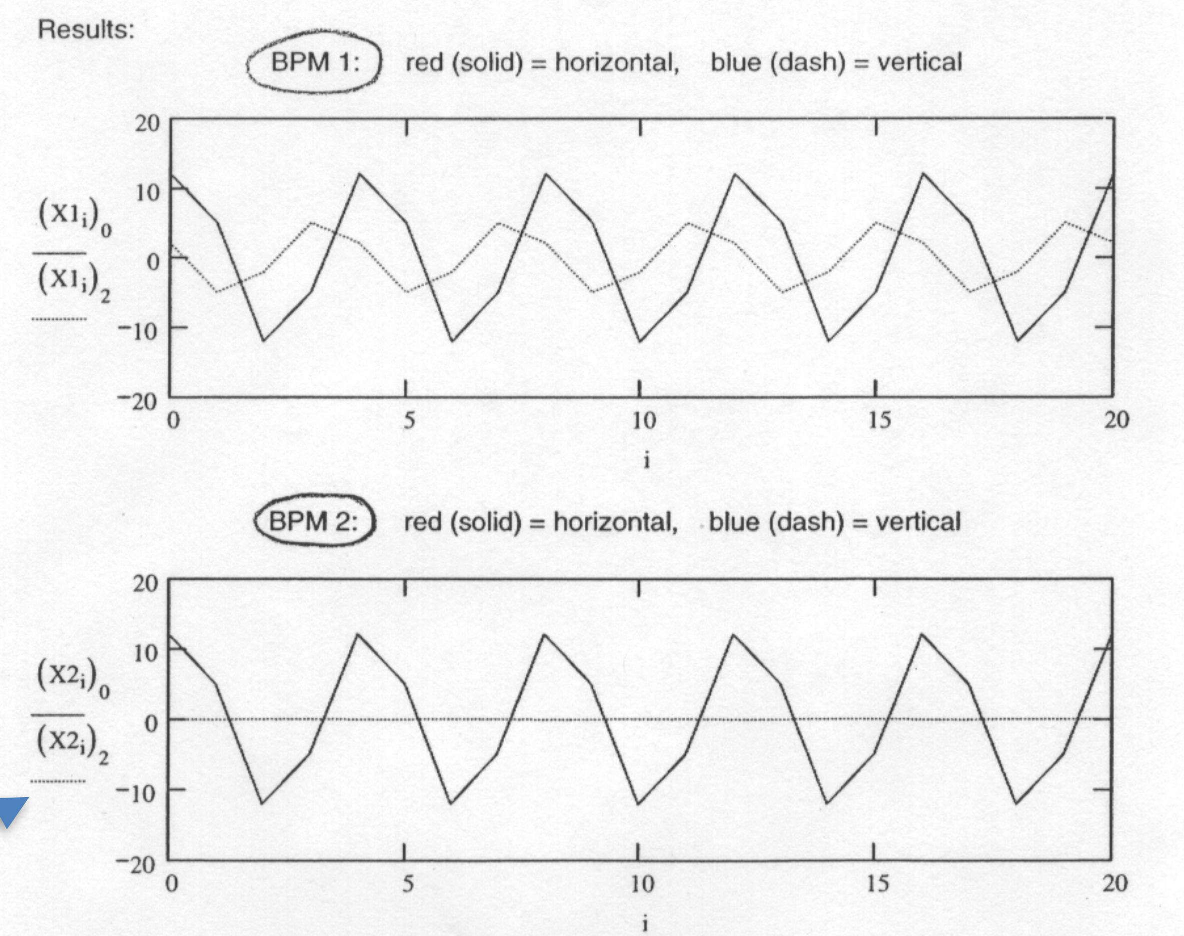

(a simple example)

Coupled Tevatron

In early 2000's, Tevatron measurements of the minimum tune split showed that there was a strong source of coupling somewhere. Where?? So, went looking for the source(s)…

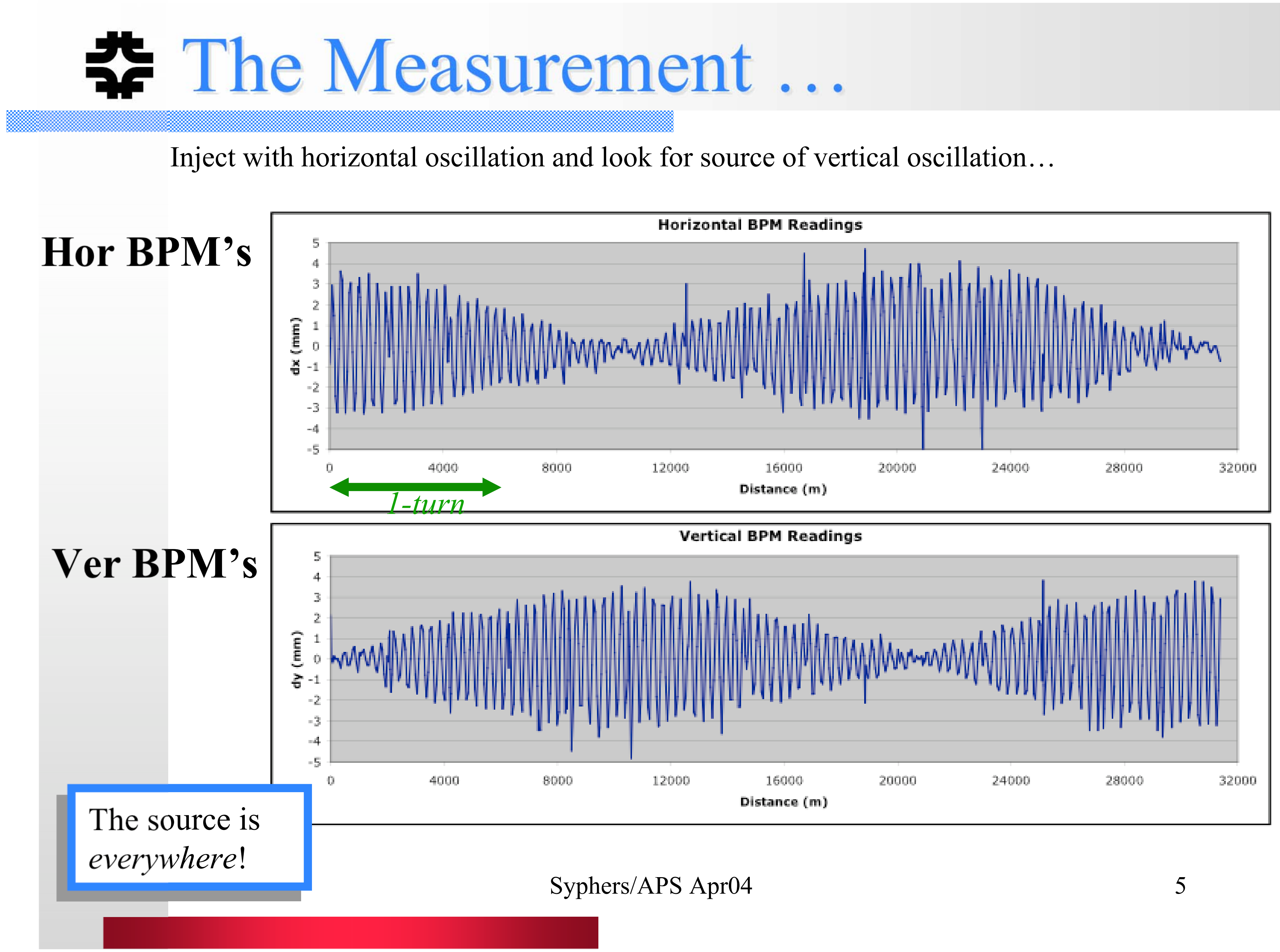

Coupled Tevatron

Tevatron Dipole

“Smart Bolts”

G-11 spacers

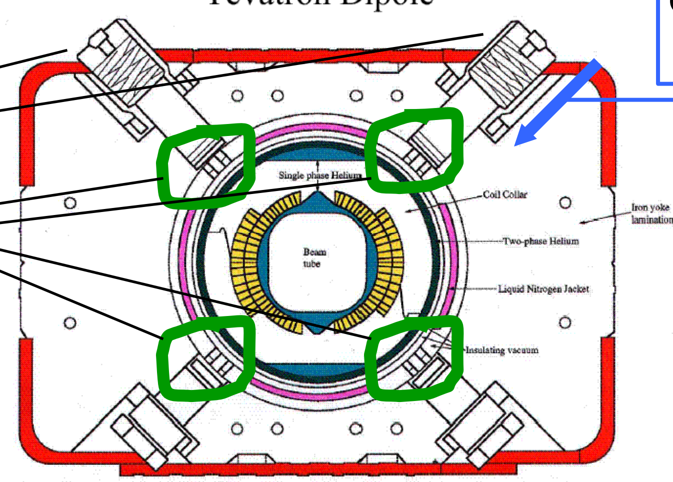

Compressed by
6 mil (0.006 in.)

$\Delta = 4.2$ mil

Spacers compressed over time, and coils became displaced by ~ 4.2 mil

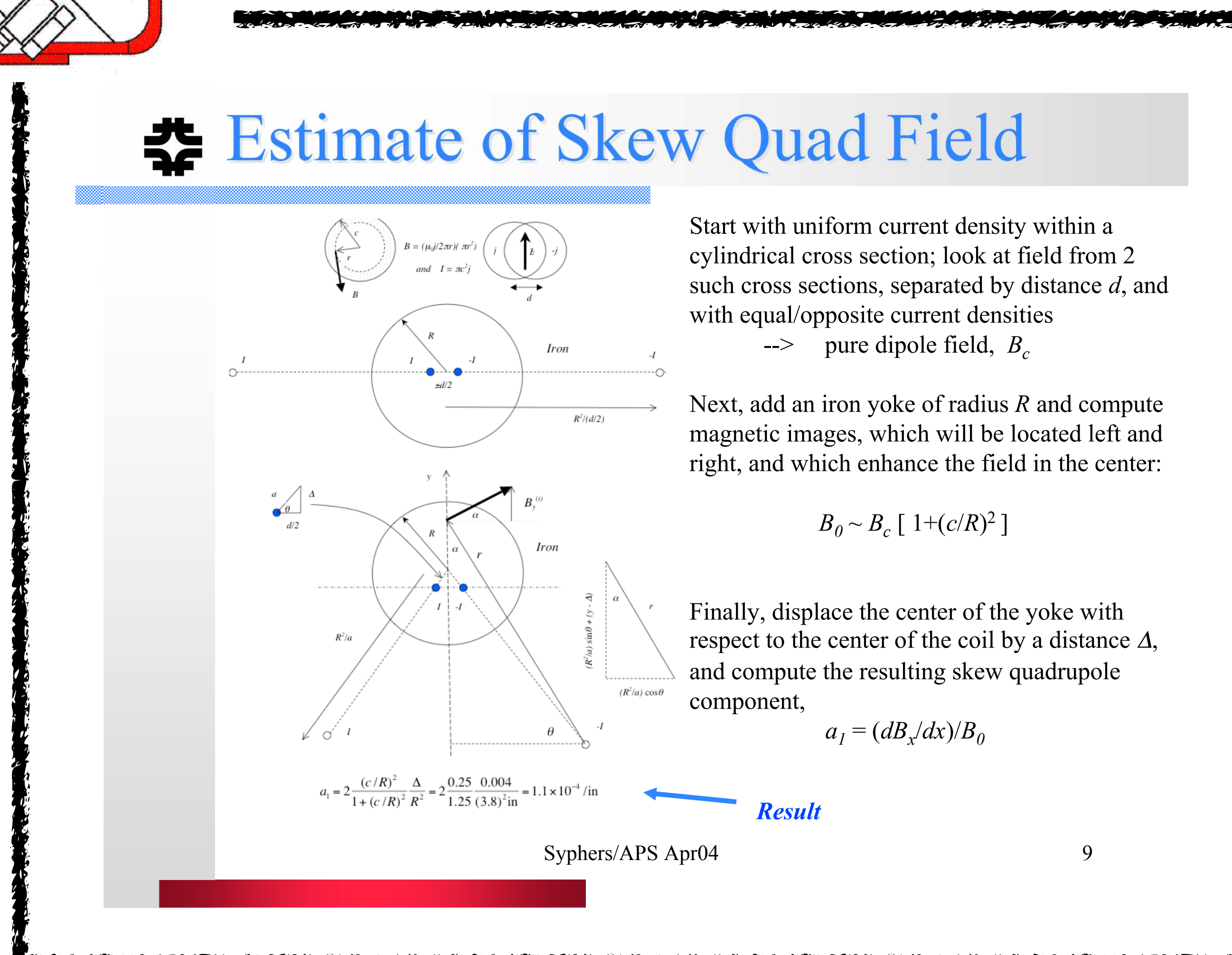

The coupling was explained as a long-term relaxation of the coils within the Tevatron dipole magnets

Emittance Measurements

2D:

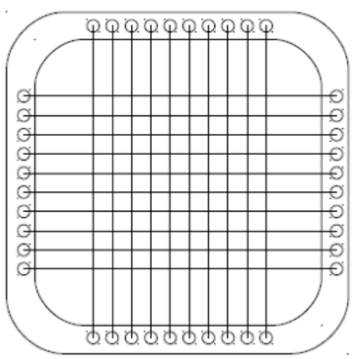

Source: M. Olvegard, *Beam Diagnostics* NPAS 2015

SEM Grid

Source: Koziol, 1998

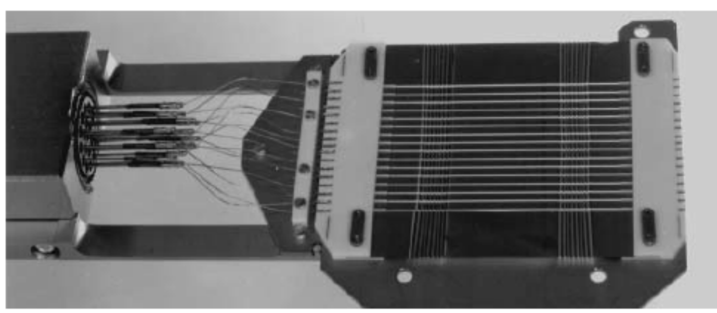

Wire Scanner

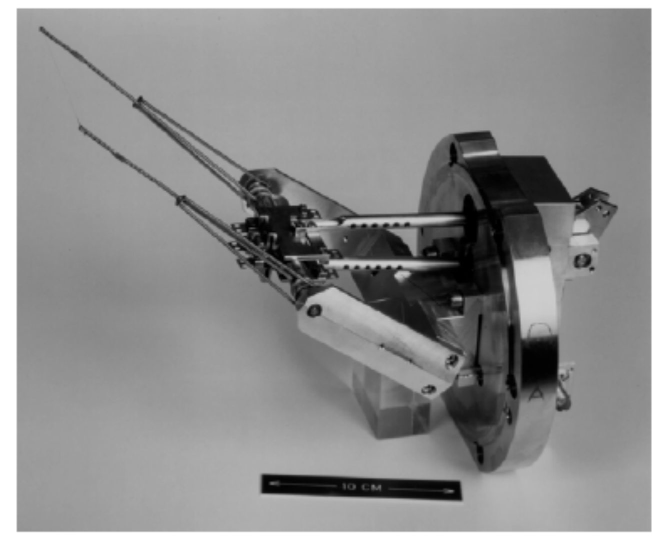

Source: Koziol, 1998

Scintillator Screen

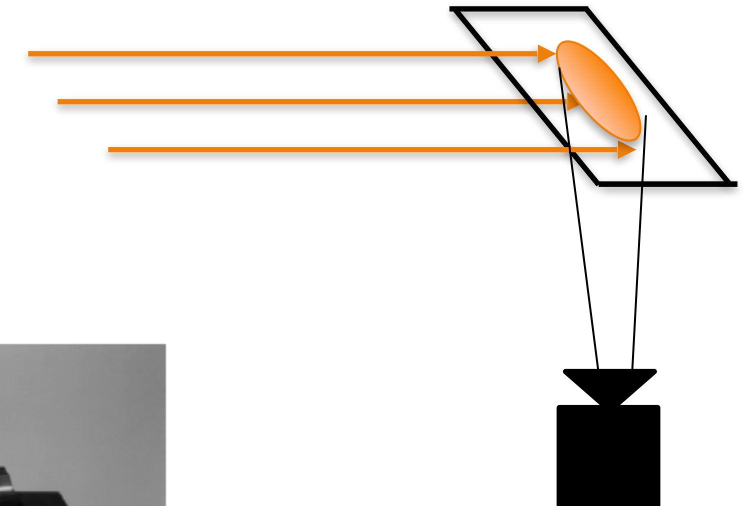

- Pepper Pot Measurement
- Allison Emittance Monitor
- Multiple profile measurements
- Quad Scan

Many emittance measurement techniques are destructive, or, at best, *disruptive*

Pepper Pot

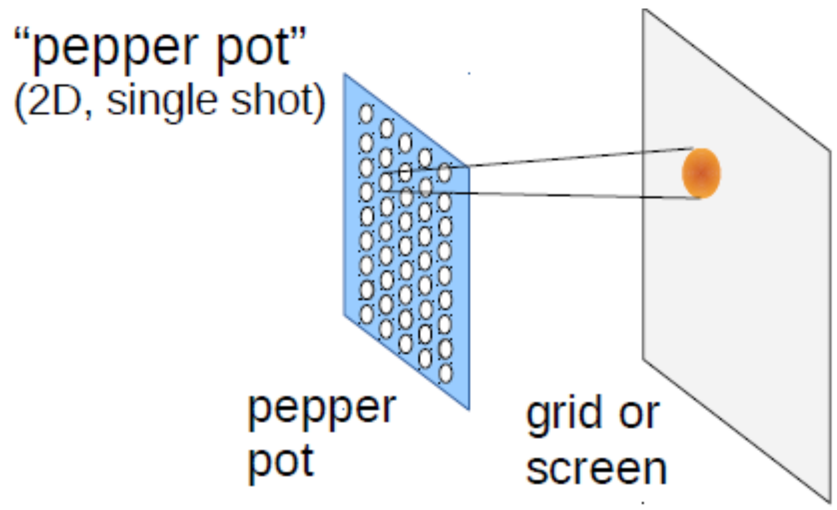

- Use a plate with small holes
- Spots appear on MCP or screen
- Measure image with CCD
- Requires high resolution profile measurement

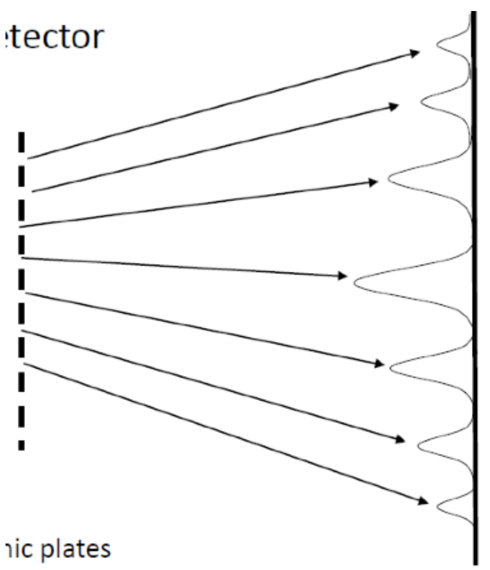

Source: M. Olvegard, *Beam Diagnostics* NPAS 2015

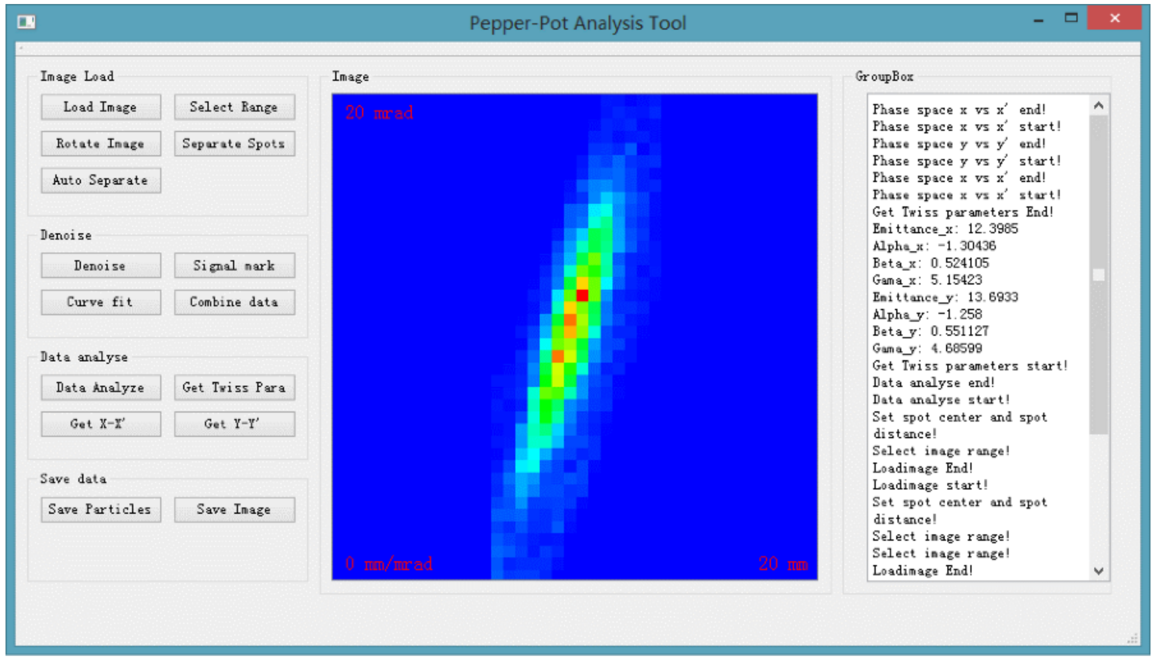

D. Wang, MSU

- Used mostly at low energy/intensity, large beams

Allison Emittance Monitor

P. Allison, J. Sherman, D. Holtkamp
IEEE Transactions on Nuclear Science, NS-30 (1983), p. 4

- Vary position of the monitor, *x*, and adjust voltage *V* to determine *x'* at that value of *x*:

$$x' = \frac{V}{W}\frac{L_p}{4g}$$

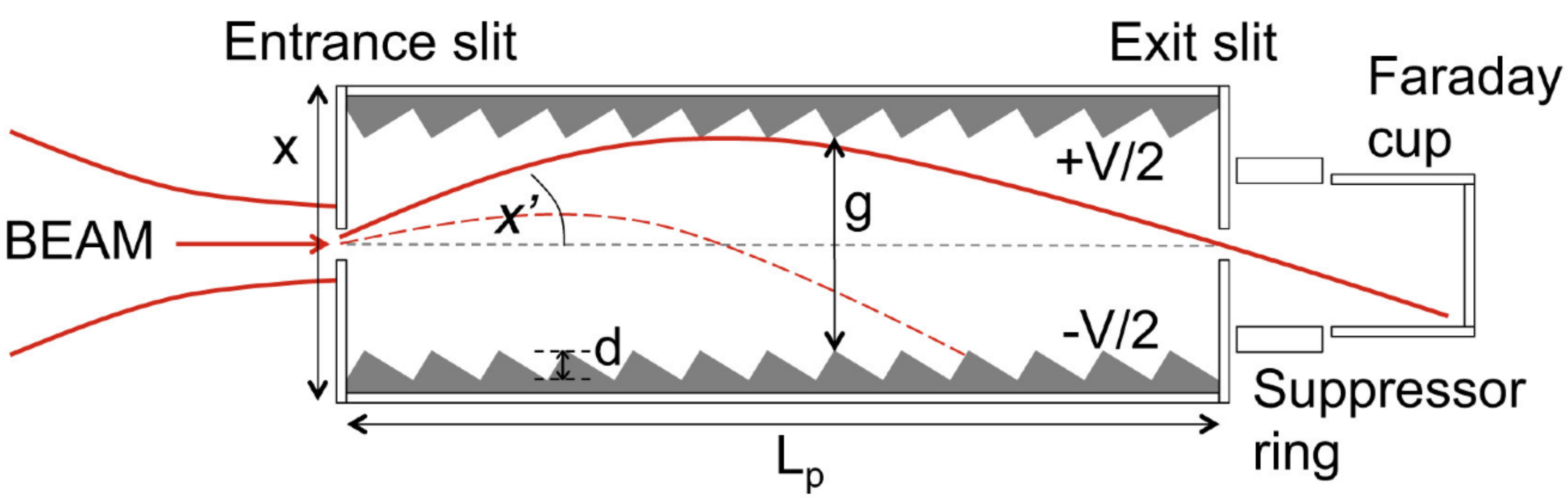

*R. D'Arcy, et al., NIM-A, **815**, 7-17 (2016)*

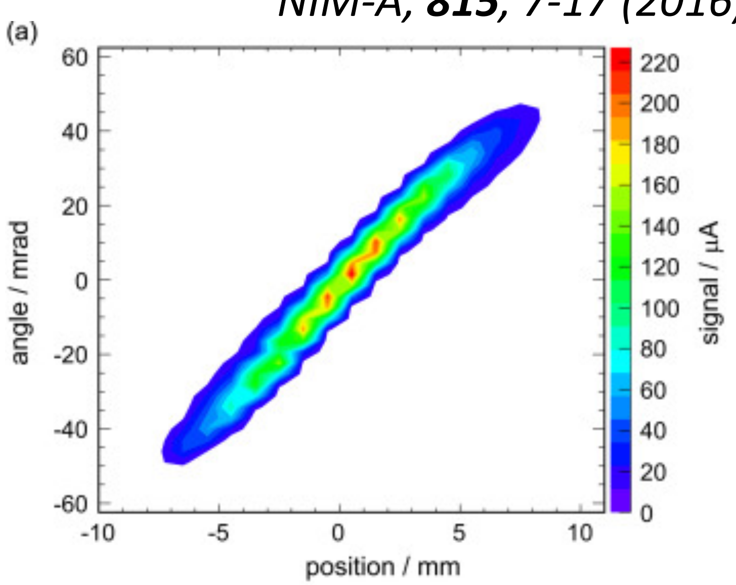

- Thus, map out *x*-*x'* phase space

Multiple Profile Measurements

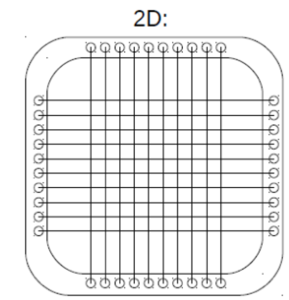

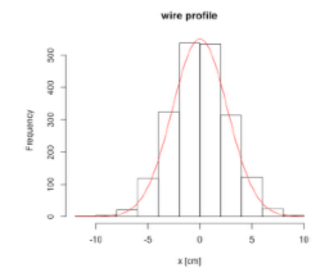

- Measure beam profile three times near a waist:

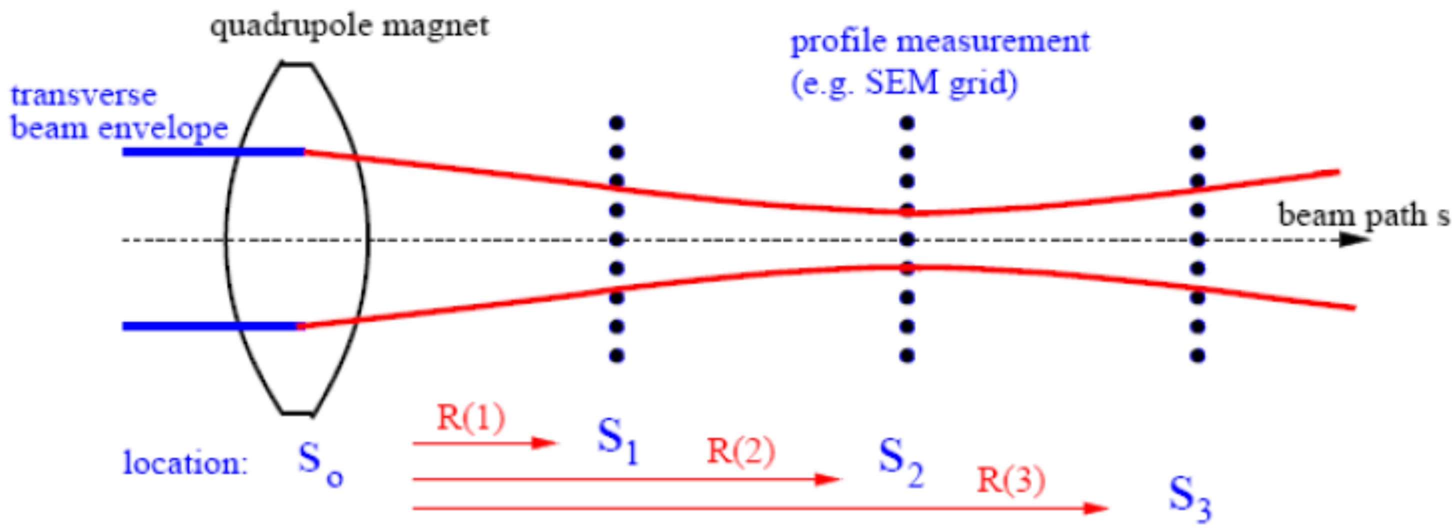

- Known matrix:
  - *R* = func(Quad Strength, distance)
- Measure:
  - *x* widths at grids
- Invert matrix to get *x,x'* correlations at s_o —> emittance

Measure

Vary *s*

Find

$$\begin{pmatrix} \langle x^2\rangle_1 \\ \langle x^2\rangle_2 \\ \langle x^2\rangle_3 \end{pmatrix} = R(s_1, s_2, s_3) \begin{pmatrix} \langle x^2\rangle_0 \\ \langle x' x\rangle_0 \\ \langle x'^2\rangle_0 \end{pmatrix}$$

Quadrupole Scan

- Instead of using three lengths, use three quad strengths!

Measure — Vary s — Find

$$\begin{pmatrix} \langle x^2 \rangle_1 \\ \langle x^2 \rangle_2 \\ \langle x^2 \rangle_3 \end{pmatrix} = R(q_1, q_2, q_3) \begin{pmatrix} \langle x^2 \rangle_0 \\ \langle x' x \rangle_0 \\ \langle x'^2 \rangle_0 \end{pmatrix}$$

- Still fully determined, but only one detector needed.
- With more than 3 measurements, do least squares optimization

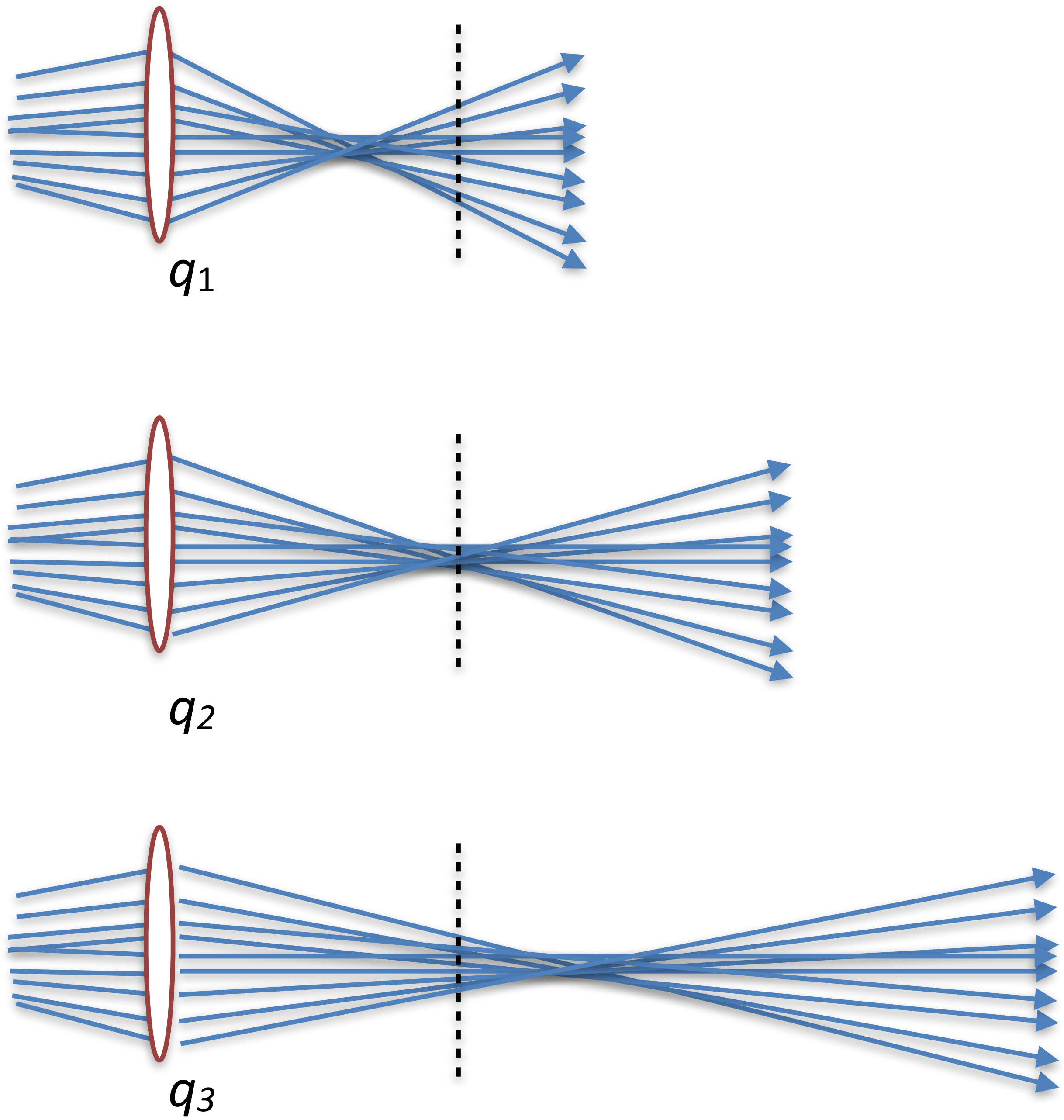

Emittance Measurements

- Tomographic Techniques

Longitudinal Profiles

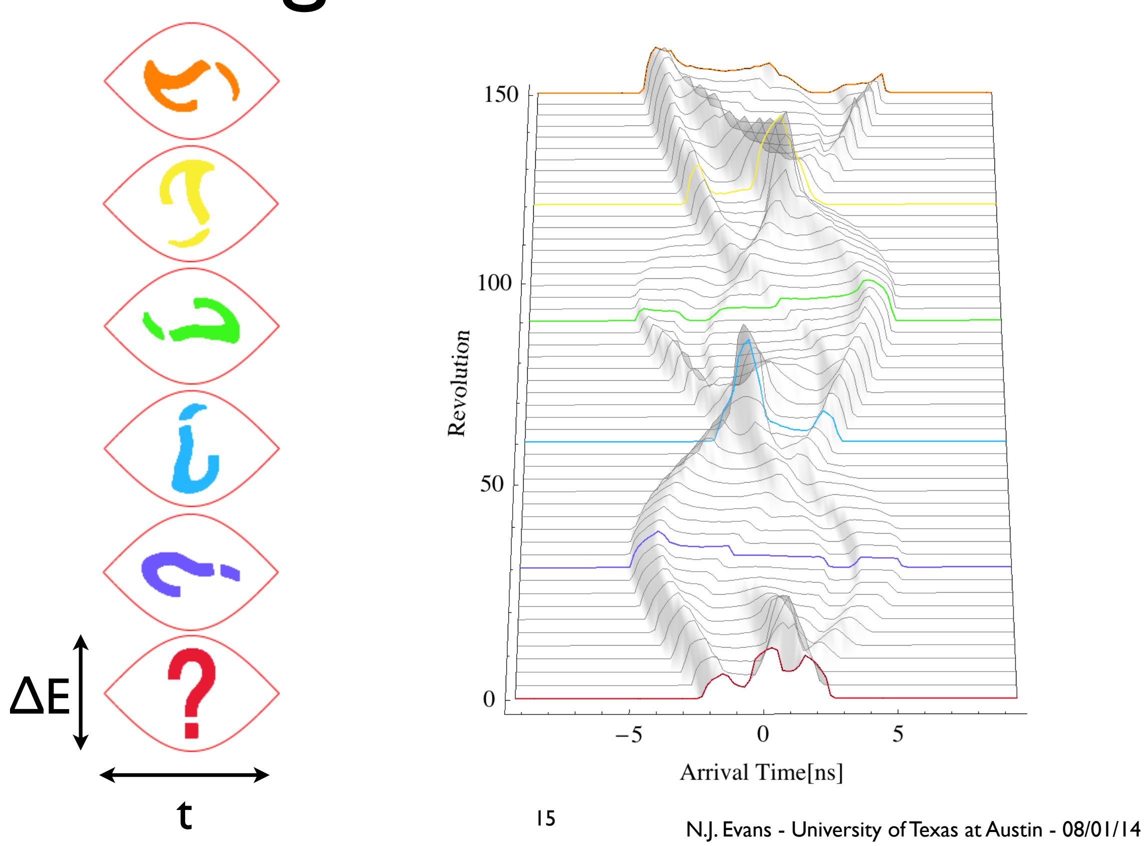

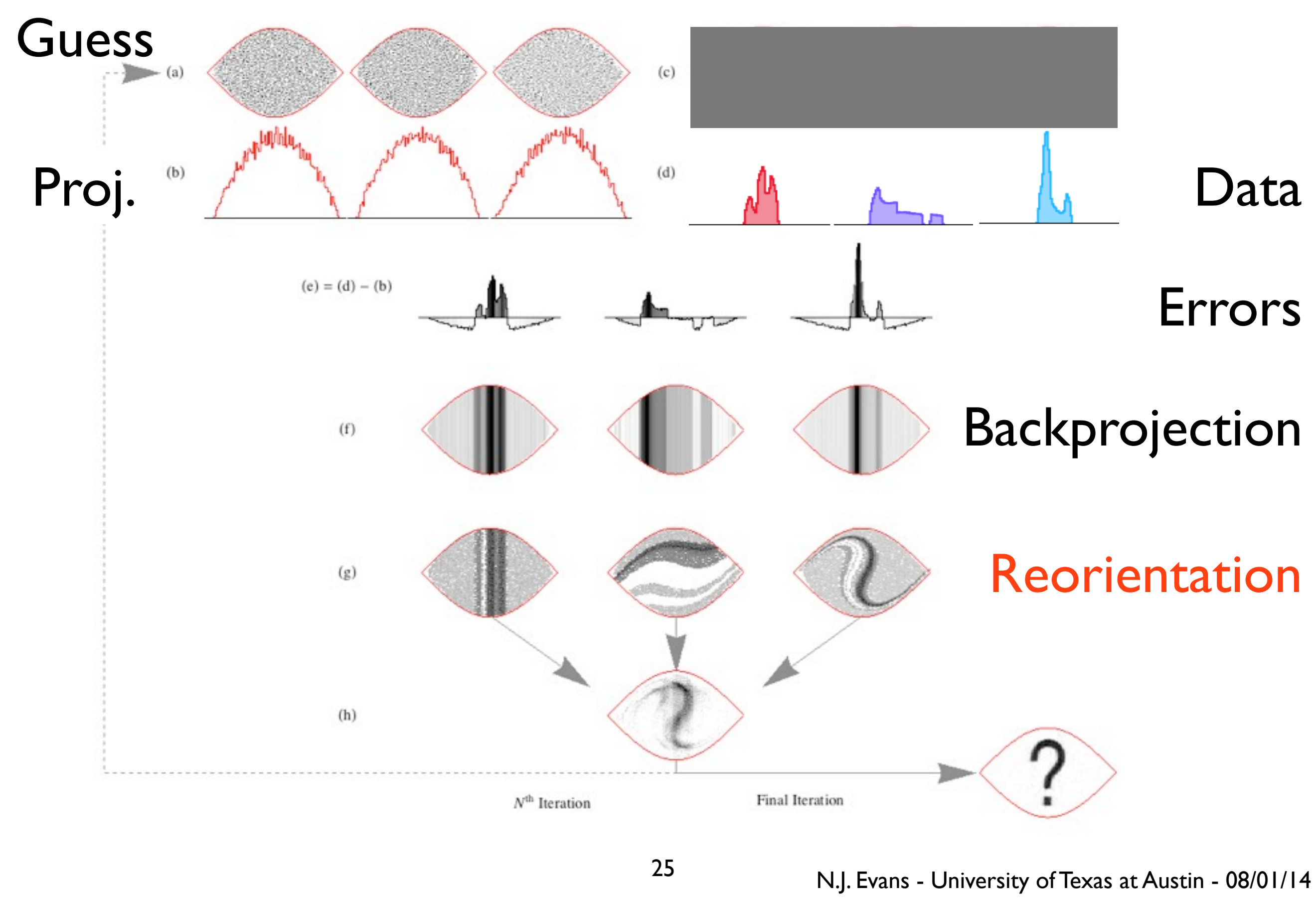

Longitudinal Tomography

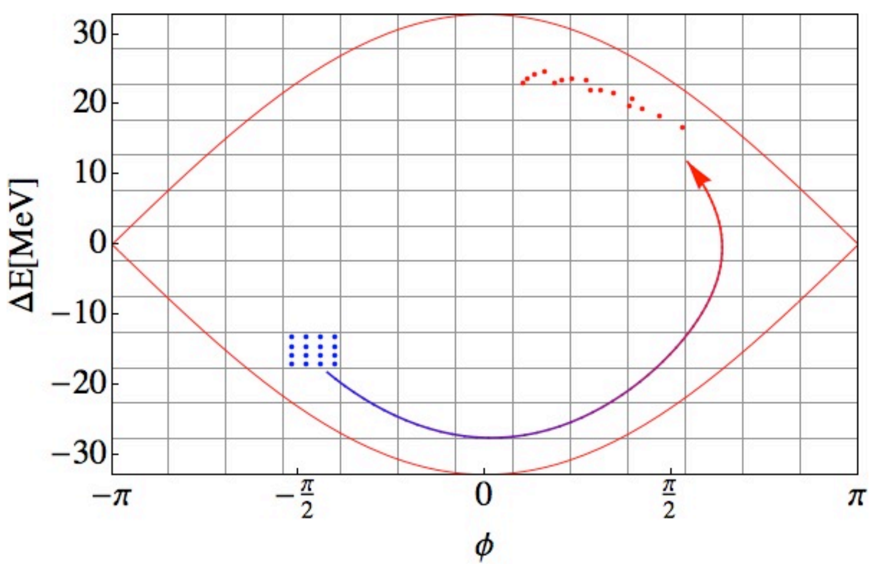

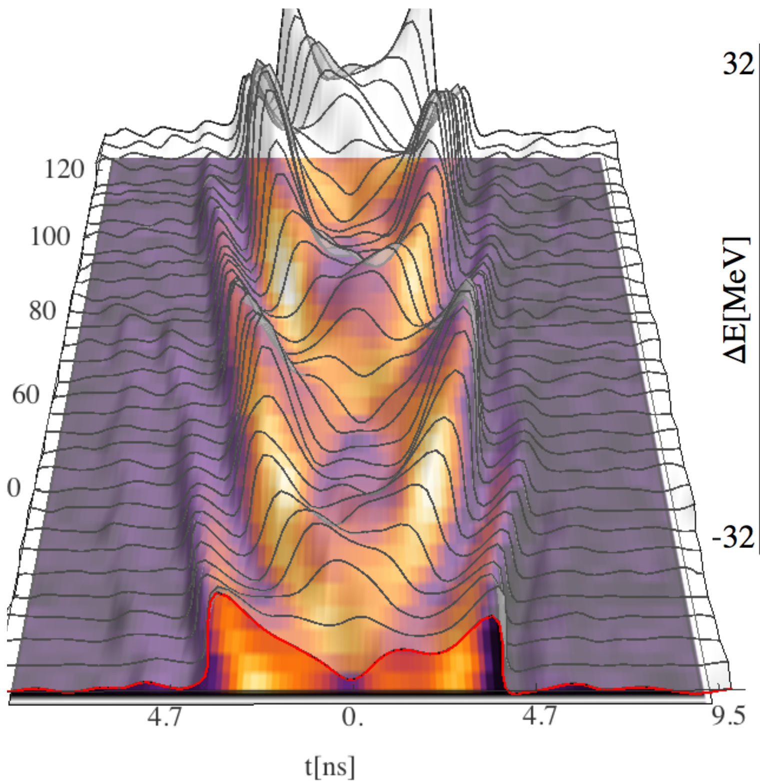

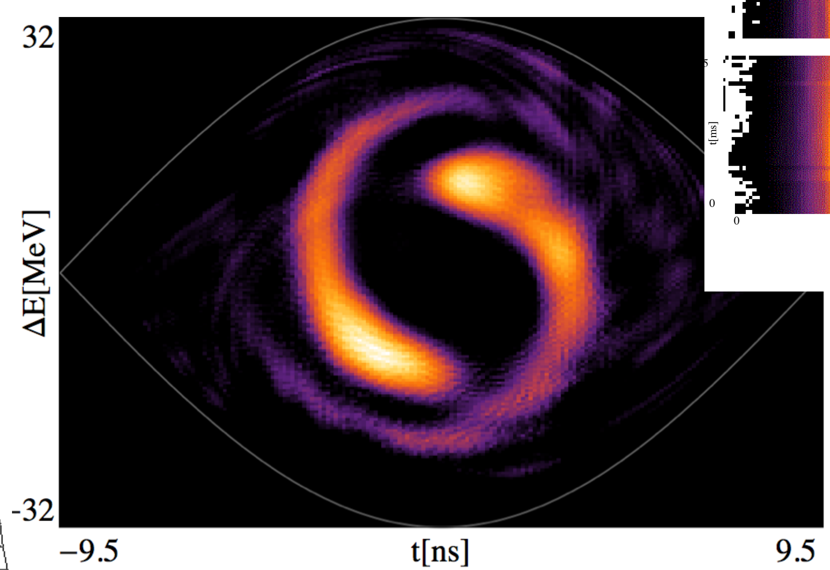

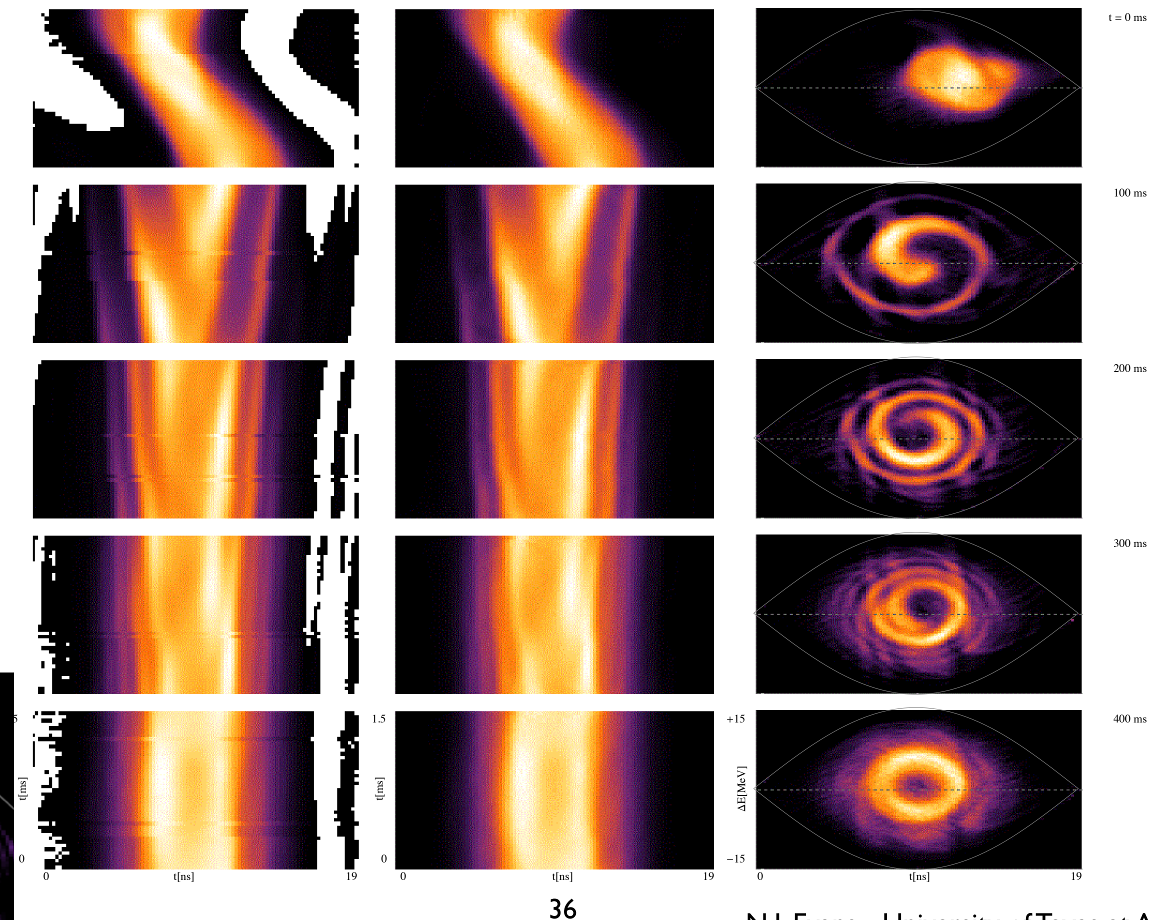

N.J. Evans - University of Texas at Austin -

Measuring Transverse Phase Space Motion

- Beam Position Monitors
  - compare voltages induced on plates as particles pass by
  - essentially,
    - dx ~ (R-L) / (R+L)
    - with corrections
- Modern electronics allow for turn-by-turn measurement at many locations
- Two BPM's near each other can give phase space info

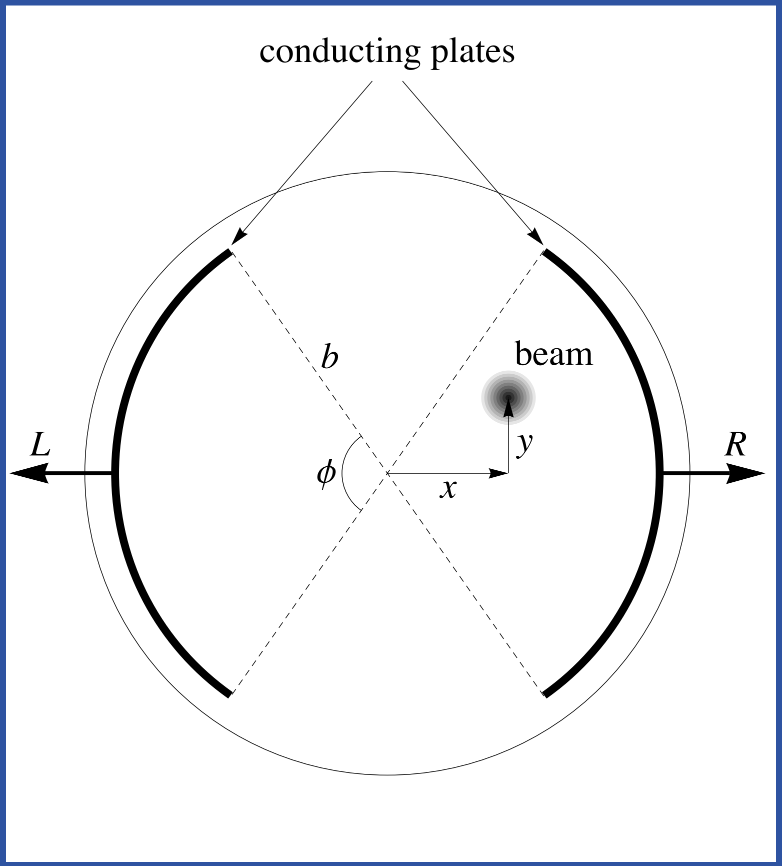

if know M between locations 1 and 2:

$$\begin{pmatrix} x \\ x' \end{pmatrix}_2 = M \begin{pmatrix} x \\ x' \end{pmatrix}_1$$

then, if measure x_1 and x_2, can determine x'_1

Fermilab

Early Tevatron Measurements

- First used a turn-by-turn BPM system for phase space measurements in 1985
- Use two BPMs with known optics between them to determine both *x* and *x'* at a single location

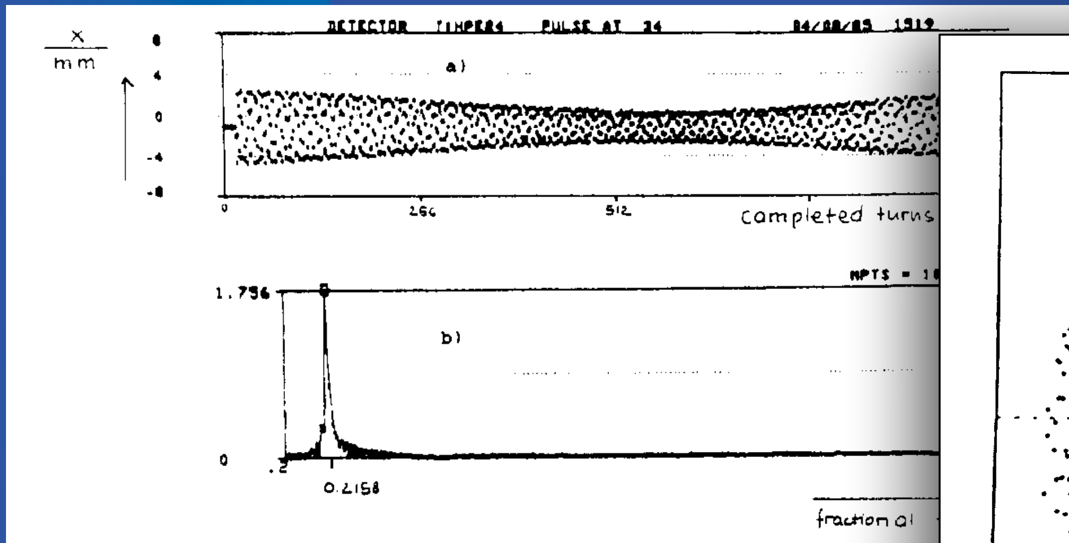

FIGURE 2 a)The beam position at one of the horizontal detectors on 1024 successive turns. dot is a measurement taken every 21 μs. b) The Fourier spectrum of fig. 2a.

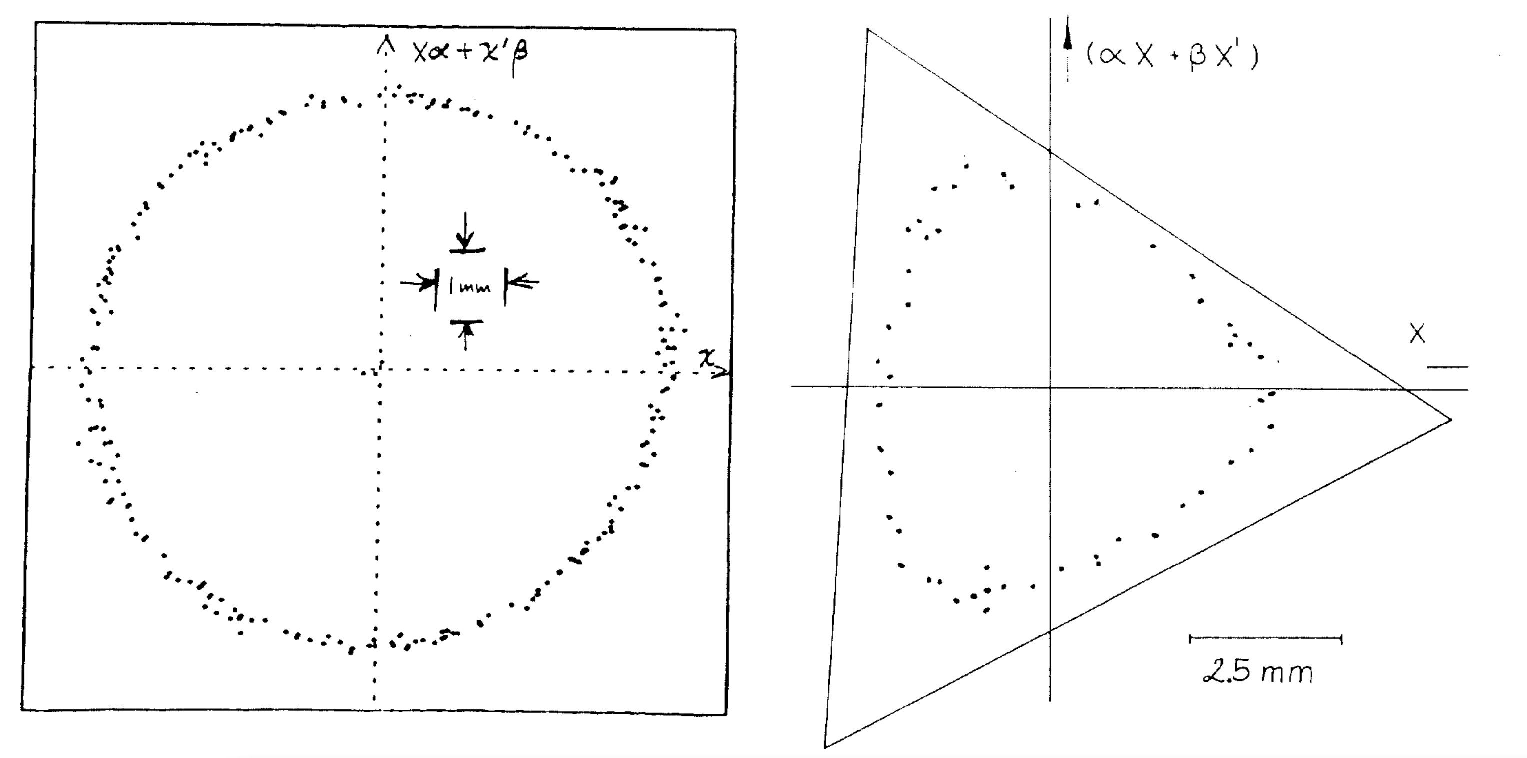

Figure 3. Me
horizontal b
is about 4 m
of beam.

Figure 4. Similar to Figure 3 except that the horizontal tune is near 19.33 and sextapoles have been energized.

D.A. Edwards, *et al.*, *Part. Accel.* Vol. 19, No. 1-4, p.145 (1986)

Fermilab

As Viewed in Phase Space

- Distribution is purposely displaced using a “kicker” magnet
- Particles oscillate at different rates, depending upon their amplitude, or their momentum (or both)
- the “center-of-mass” as measured by the BPM tends to zero

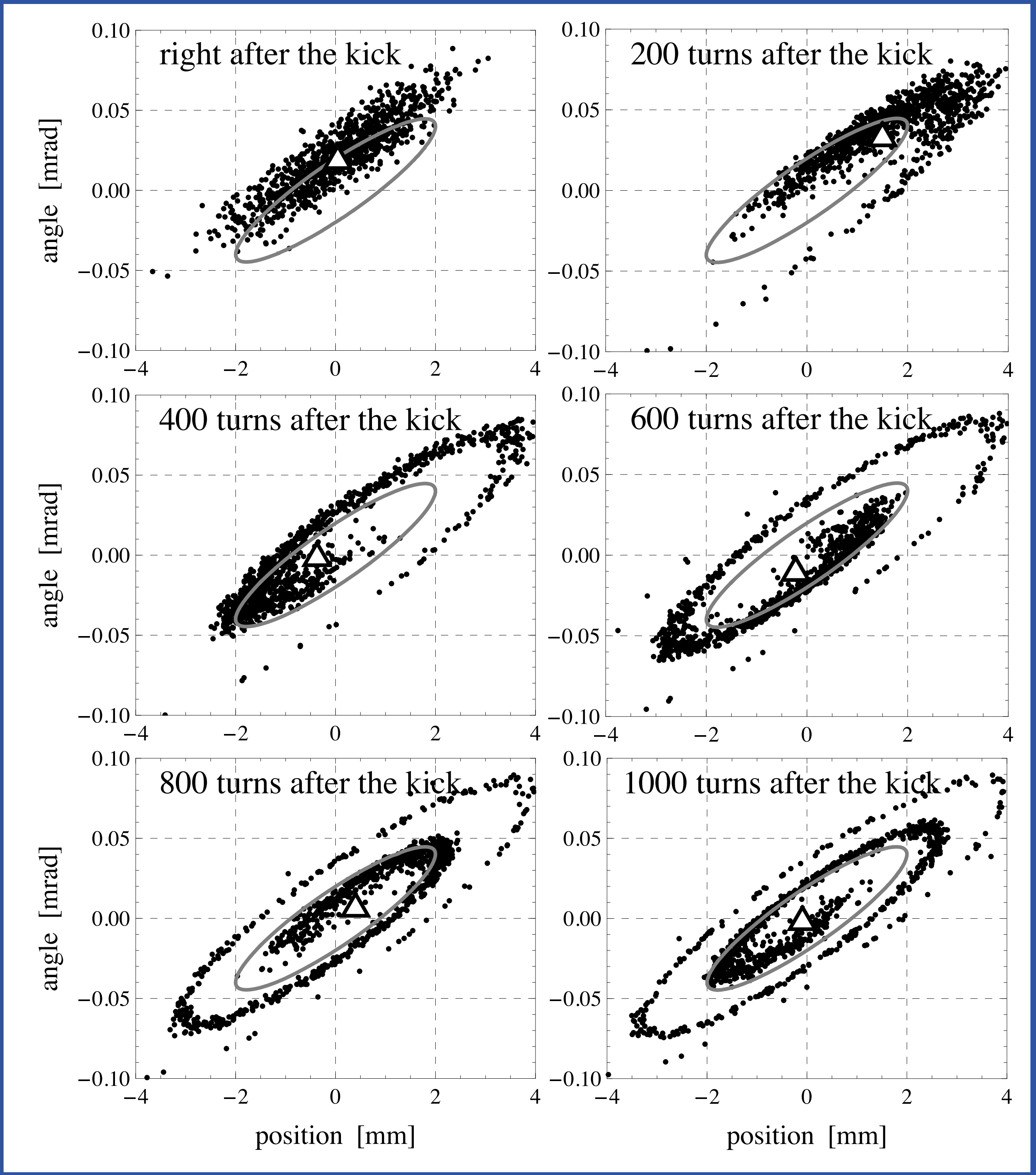

Tune Spread

Observe the motion at one point in ring, "kick" the beam

- Momentum spread due to chromaticity
  - "natural" effect; also driven by field errors in magnets ~ x^2
- Nonlinear tune spread
  - field terms ~ x^2, x^3, etc.
- Tune spread generates a "decoherence" of beam position signal

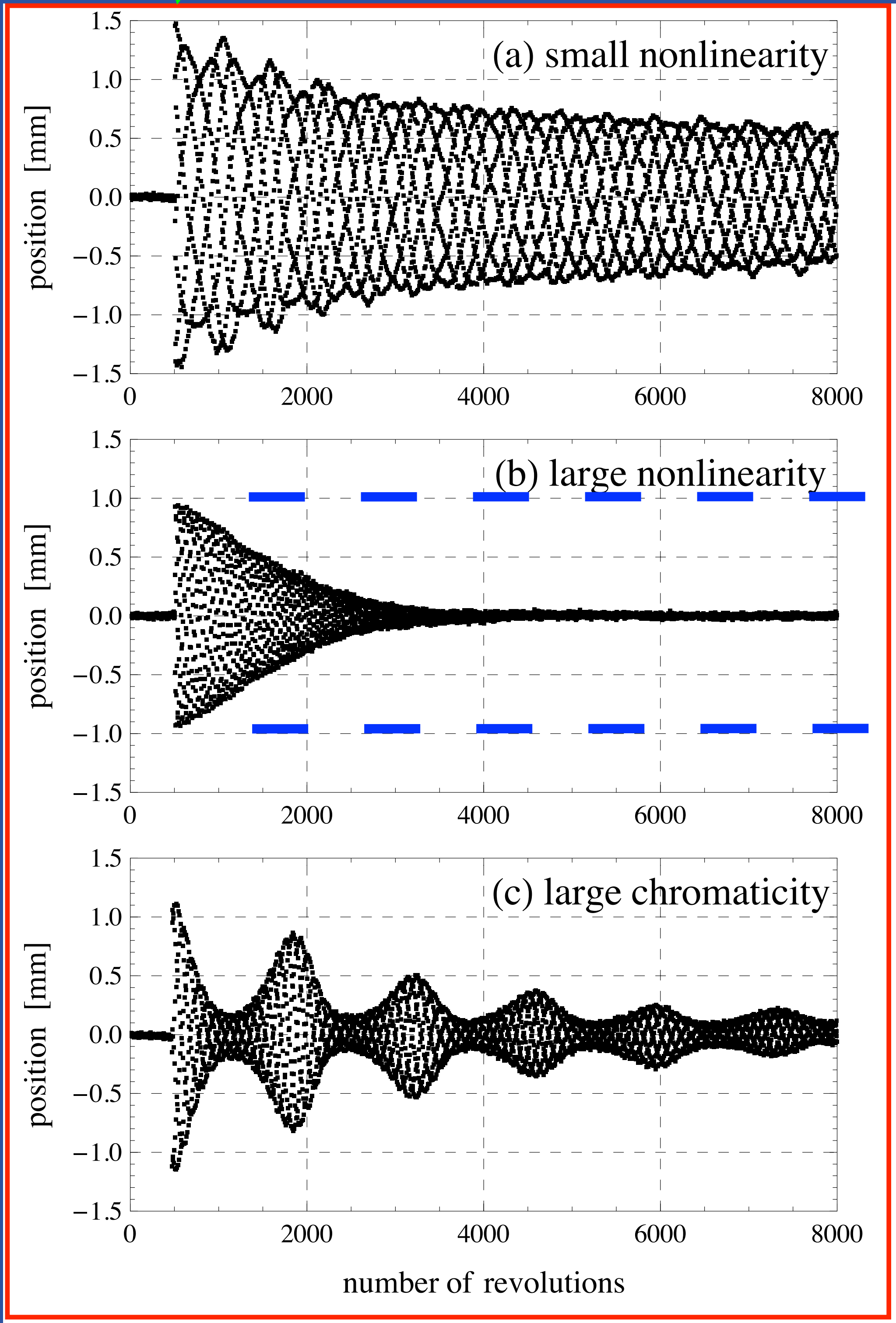

Fermilab

Arriving at Single Particle Motion from a Beam

- Characteristics of the signal can be parameterized in terms of...
  - initial kick amplitude, a
    - relative to rms size
  - relative momentum spread
  - tune vs. amplitude
    - coefficient; $\nu \sim a^2$
  - oscillation frequency of longitudinal motion
  - ideal linear oscillation frequency

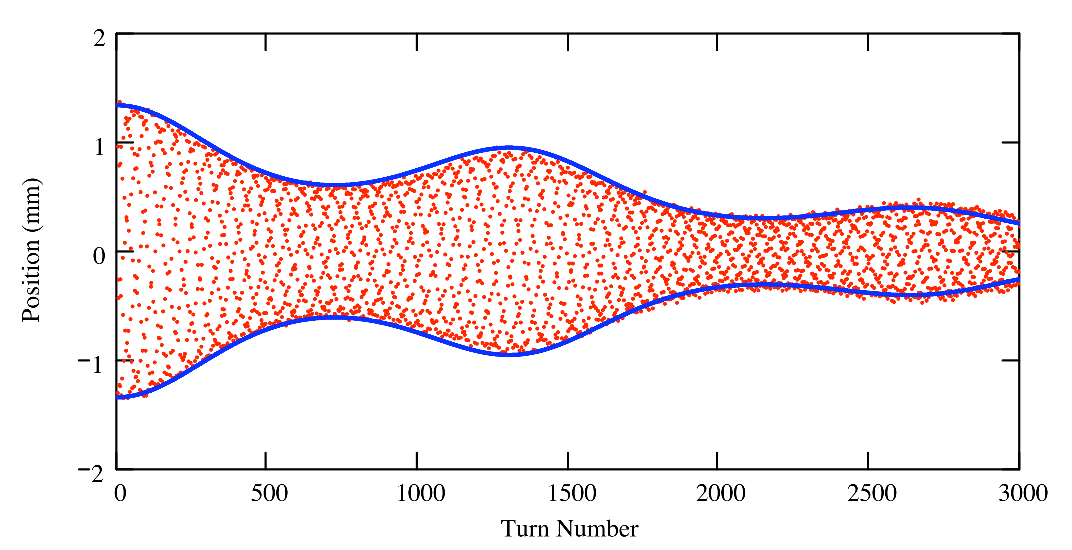

$$\overline{x}(n) = a \cdot e^{-[2\sigma_s \xi \nu_s^{-1} \sin(\pi \nu_s n)]^2/2} \cdot \left(\frac{1}{1+(\nu_p n)^2} \; e^{-\frac{a^2}{2\sigma^2} \frac{(\nu_p n)^2}{1+(\nu_p n)^2}} \right) \cdot \cos[2\pi \nu_0 n + \Delta\overline{\phi}(n)]$$

- Can thus (a) infer single particle motion over many revolutions, and (b) use these signals to tune up the accelerator for the measurement by reducing effects of momentum spread (for example)

Fermilab

Tevatron Experiment E778 (late 1980's)

- Aperture Criterion for the Superconducting Super Collider (SSC)
  - Dedicated accelerator experiment to verify predictions of computer simulations of nonlinear particle beam dynamics

Simulations:

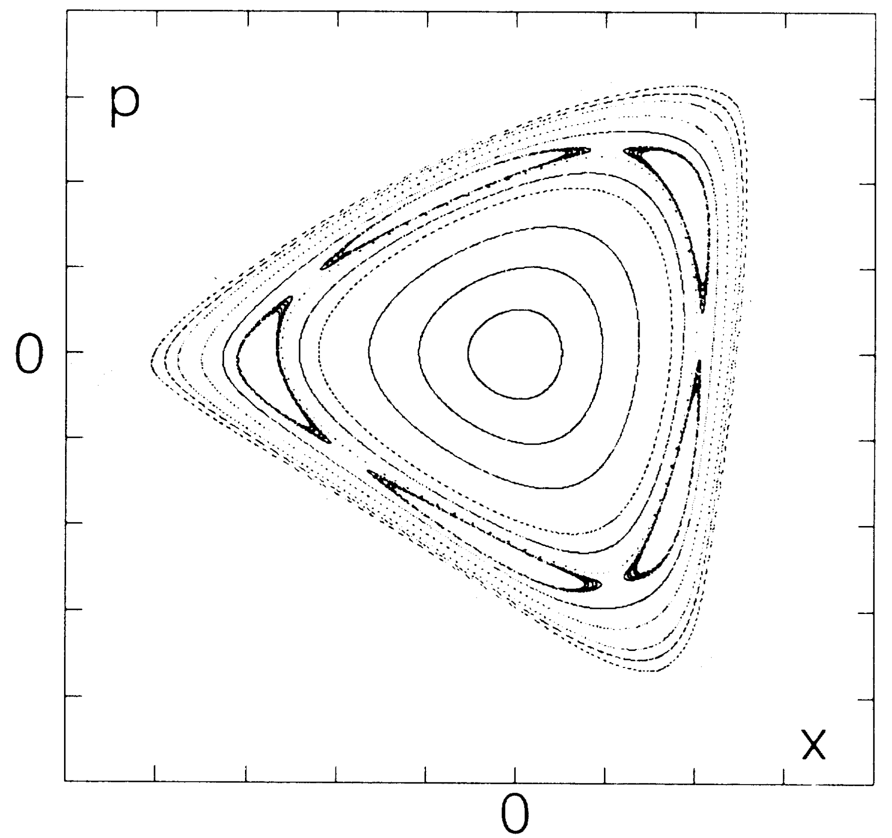

FIG. 1. Poincaré map generated by numerically tracking particles of various amplitudes. Most of the features have been demonstrated and measured.

Data:

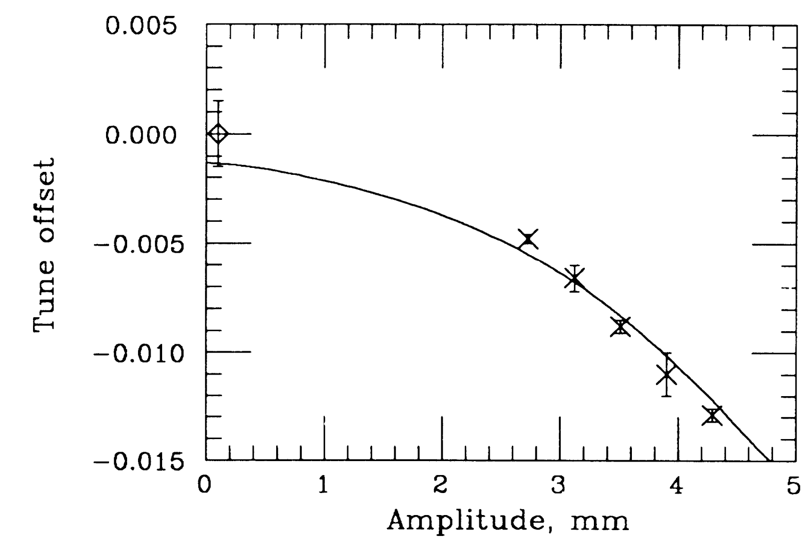

FIG. 3. Dependence of tune on amplitude. Data points are measured; the curve is predicted.

VOLUME 61, NUMBER 24 PHYSICAL REVIEW LETTERS 12 DECEMBER 1988

Experimental Investigation of Nonlinear Dynamics in the Fermilab Tevatron

A. Chao, D. Johnson, S. Peggs, J. Peterson, C. Saltmarsh, and L. Schachinger
Superconducting Supercollider Central Design Group, Berkeley, California 94720

R. Meller, R. Siemann, and R. Talman
Newman Laboratory of Nuclear Studies, Cornell University, Ithaca, New York 14853

P. Morton
Stanford Linear Accelerator Center, Stanford, California 94305

D. Edwards, D. Finley, R. Gerig, N. Gelfand, M. Harrison, R. Johnson, N. Merminga, and M. Syphers
Fermi National Accelerator Laboratory, Batavia, Illinois 60510
(Received 11 July 198)

Tevatron Experiment E778

- Direct measurement of particles trapped in resonance Islands

Data:

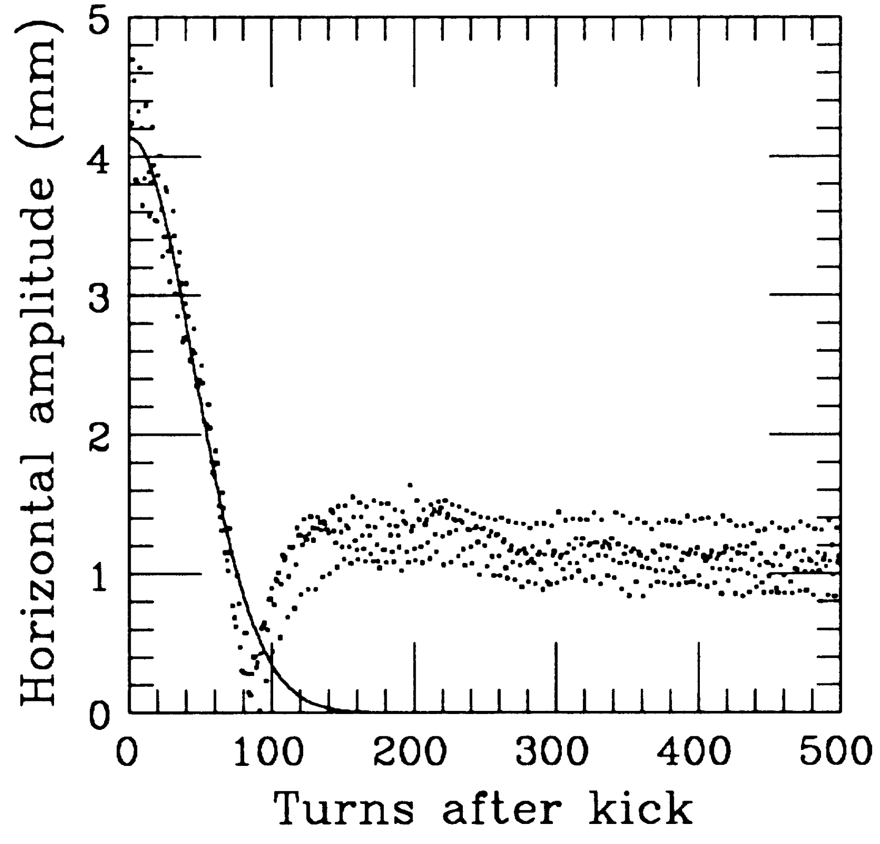

FIG. 2. Raw BPM turn-by-turn output for 500 turns after transverse deflection of the beam. The smooth fit has the theoretically expected Gaussian shape.

Data:

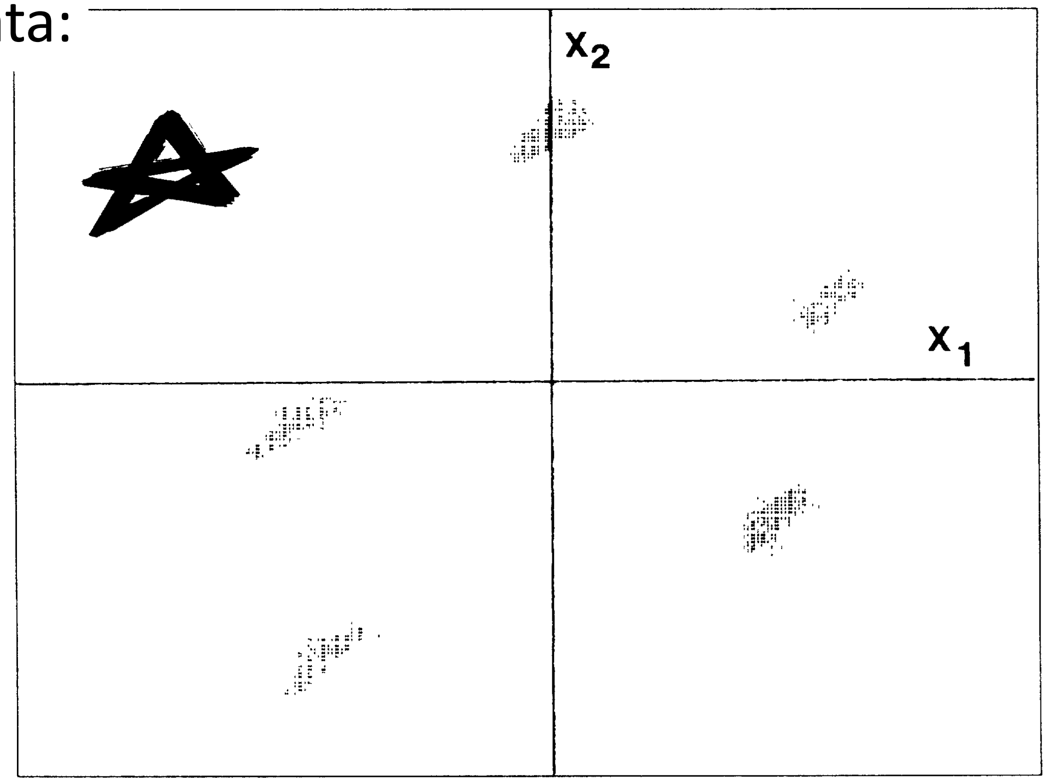

FIG. 5. "Raw experimental Poincaré map" exhibiting a metastable state of the accelerator. The "logo" in the corner of the plot is a demagnified view of the same data with successive points joined by straight lines. The point lands only on every second island, confirming the $\frac{2}{5}$ identification.

Studies at Indiana University (1990's)

- Dedicated beam physics experiments using the Indiana Cooler synchrotron (S.Y. Lee, *et al.*)
  - similar techniques employed...

tune placed near 1/3-integer

Data:

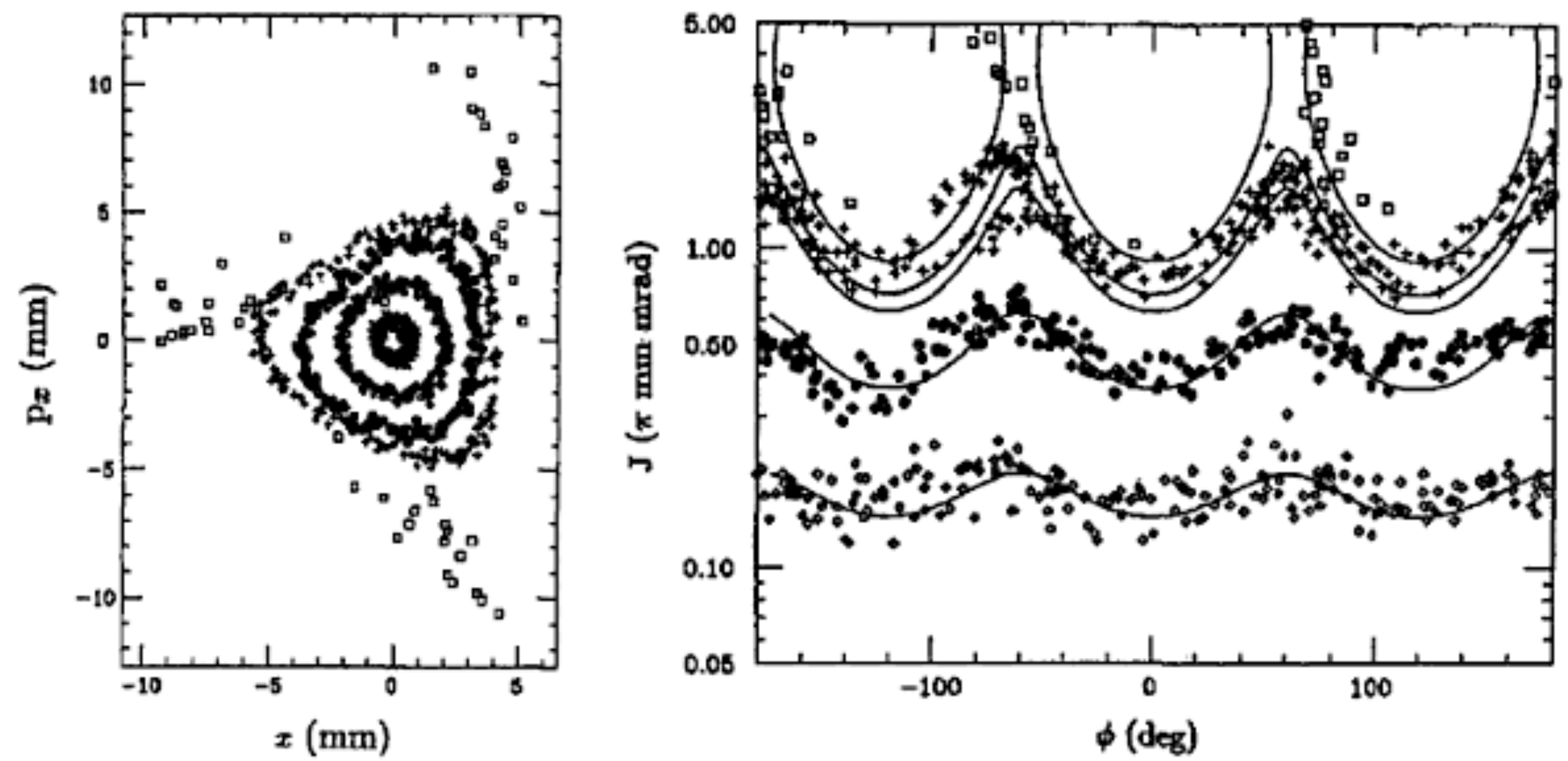

Figure 2.51: Left: The measured Poincaré map of the normalized phase-space coordinates (x, p_x) of betatron motion near a third-order resonance $3\nu_x = 11$ at the IUCF cooler ring. Note that particles outside the separatrix survive only about 100 turns. Tori for particles inside the separatrix are distorted by the third order resonance. The orientation of the Poincaré map, determined by sextupoles, rotates at a rate of betatron phase advance along the ring. The right plot shows the Poincaré map in action-angle variables (J, ϕ). The solid lines are Hamiltonian tori of Eq. (2.392).

Studies at Indiana University

- Here, betatron tune placed near 1/4-integer
  - beam position data, normalized phase space (left), action-angle phase space (right)

Data:

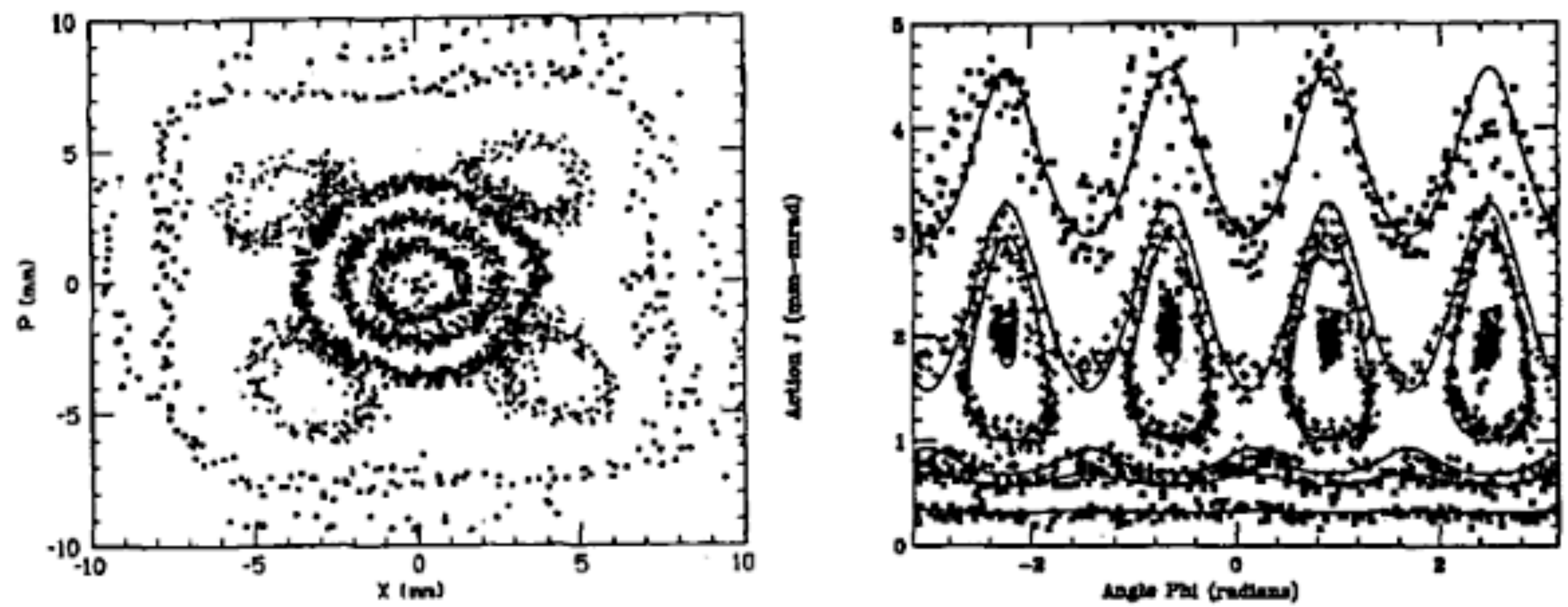

Figure 2.53: Left: The measured betatron Poincaré map (surface of section) (x, P_x) of normalized phase space near a fourth-order resonance $4\nu_x = 15$ at the IUCF cooler ring. Note that the phase-space ellipse is distorted into four island when the betatron tune sits exactly on resonance. The right plot shows the Poincaré map in action-angle variables $(J = J_x, \phi = \psi_x)$. The solid lines are the Hamiltonian tori of Eq. (2.394).

Fermilab

Island Extraction -- SpS (CERN)

(Giovannozzi, *et al.*, PAC05)

- More recently, a new technique for sending pulses of beam from the CERN SpS toward Gran Sasso (neutrino experiment)
- Form “resonance islands” and extract one-by-one toward the experiment

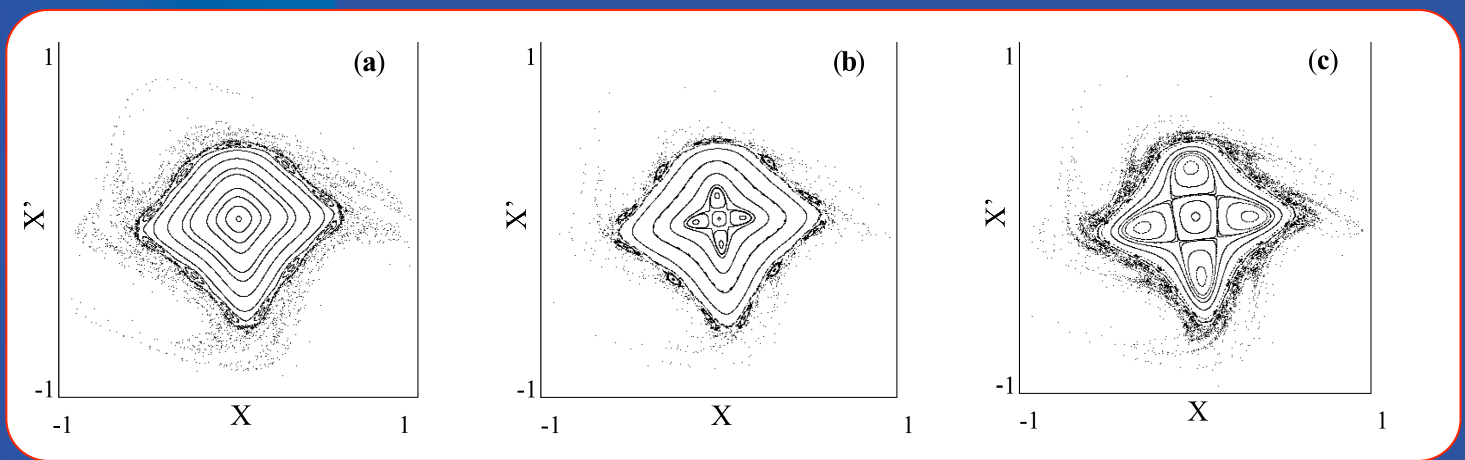

evolution of phase space topography

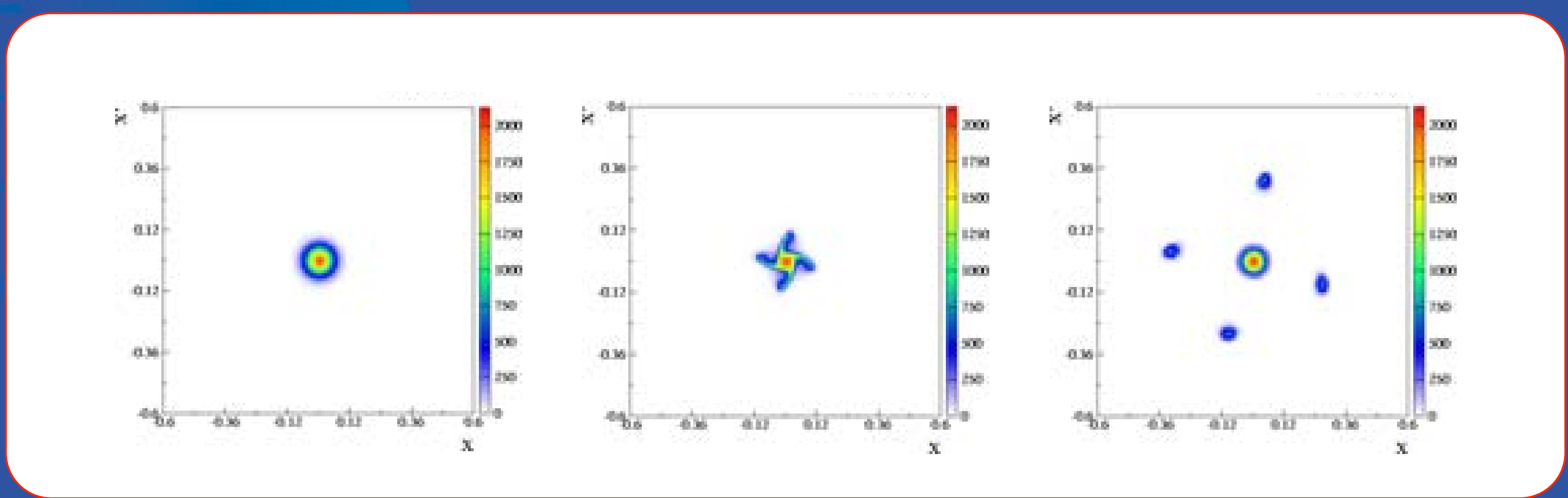

evolution of phase space distribution

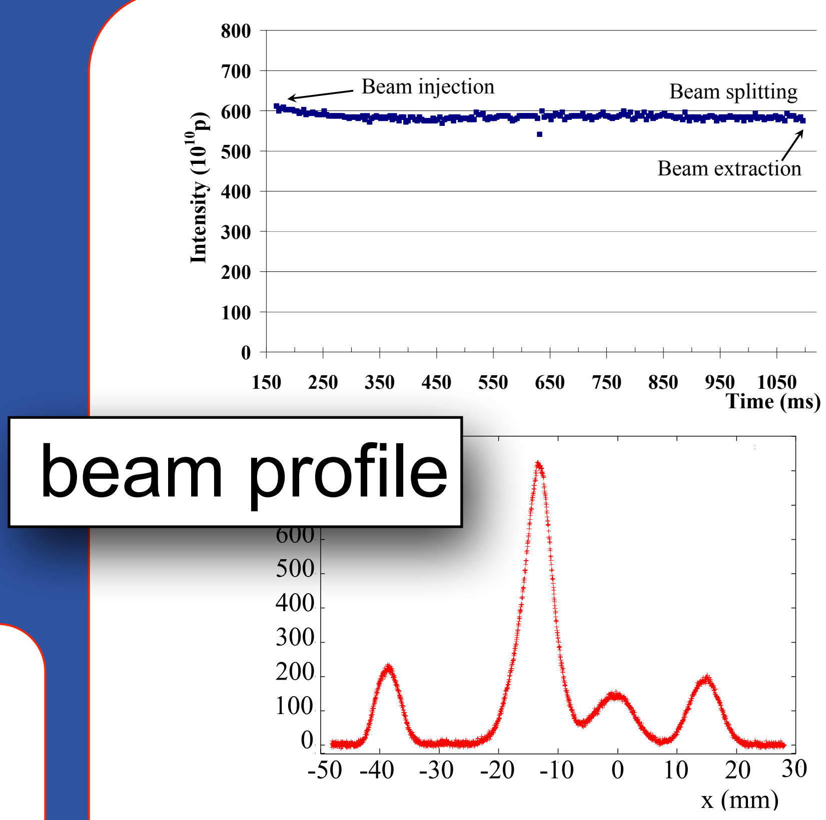

Figure 5: Best result achieved with a high-intensity beam, whose intensity as a function of time (upper) and horizontal beam profile at the end of the capture process (lower) is shown. The profile is not centred at zero due to an instrumental offset of the wire position.

Dynamic Aperture Measurements

- Early verification of nonlinear dynamics
- measured phase space; tune vs. amplitude
- measured dynamic aperture vs. predictions

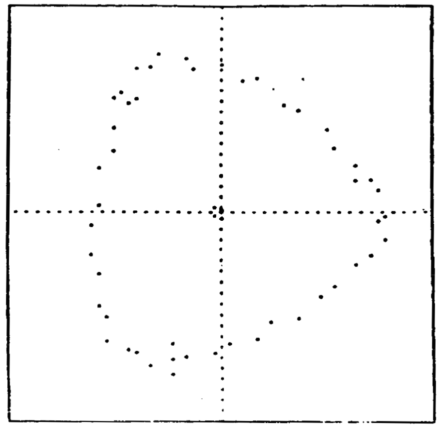

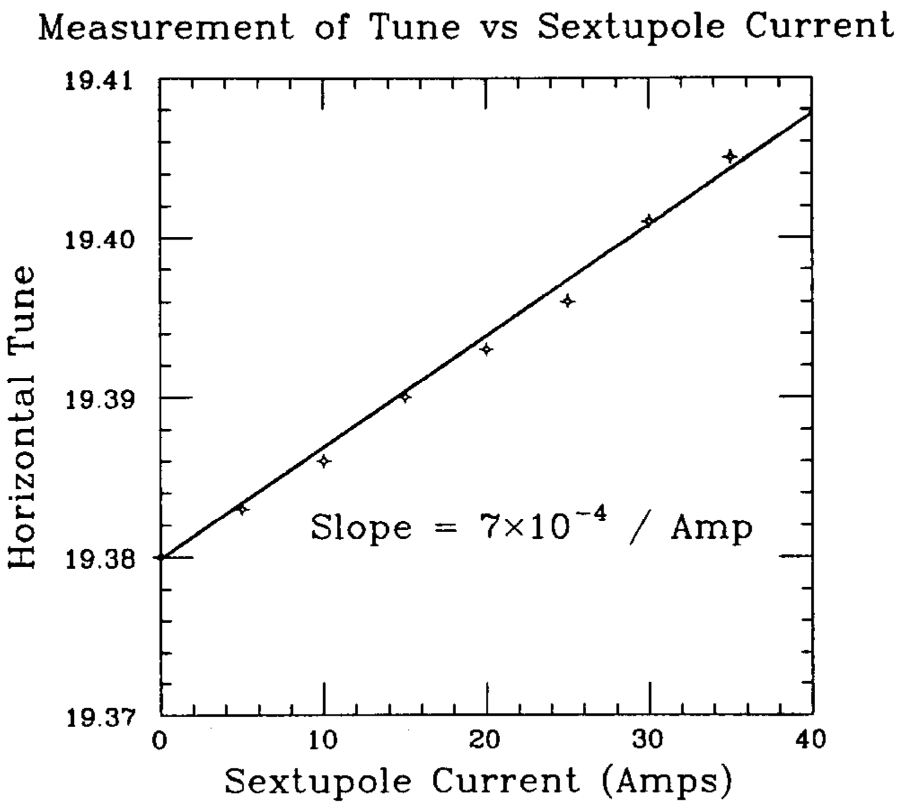

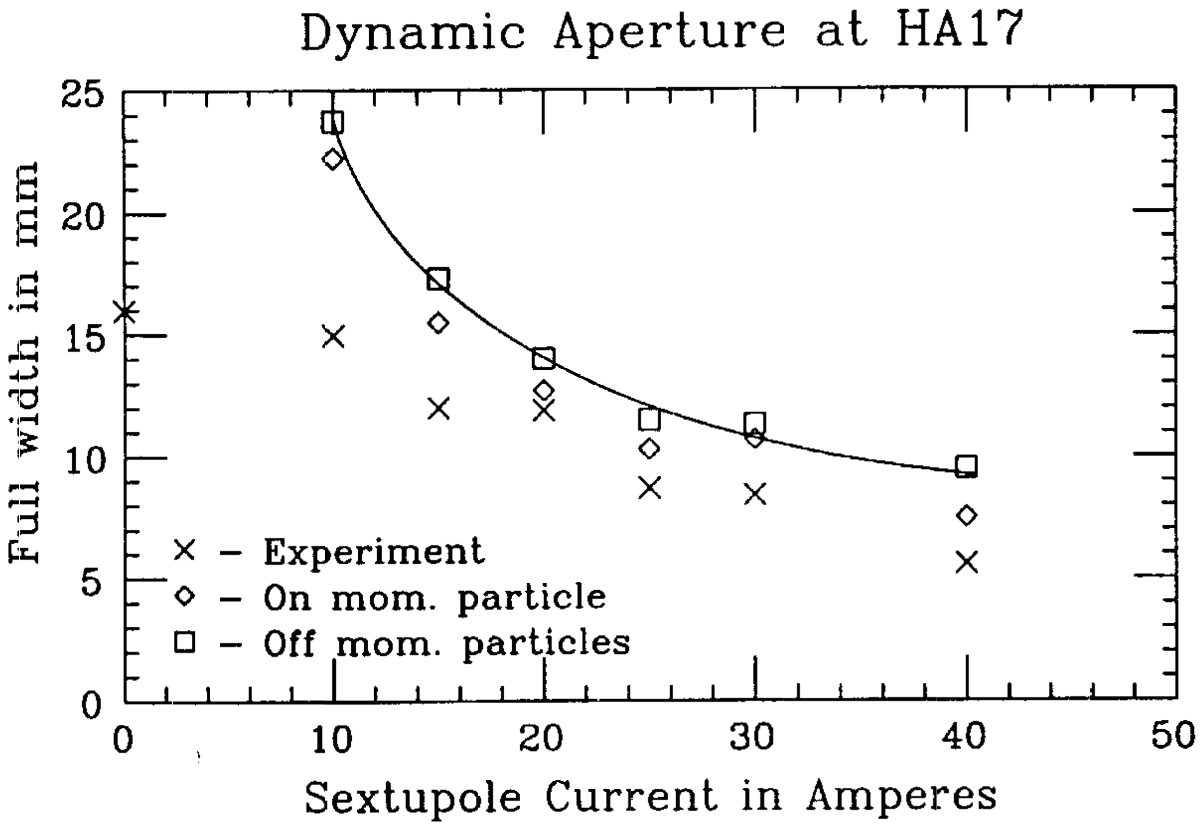

L. Merminga, et al., Tev Expt. E778

Figure 7.5: Dynamic aperture at HA17. The smooth curve is a fit to the simulated results for off-momentum particles.

LHC Dynamic Aperture Measurements

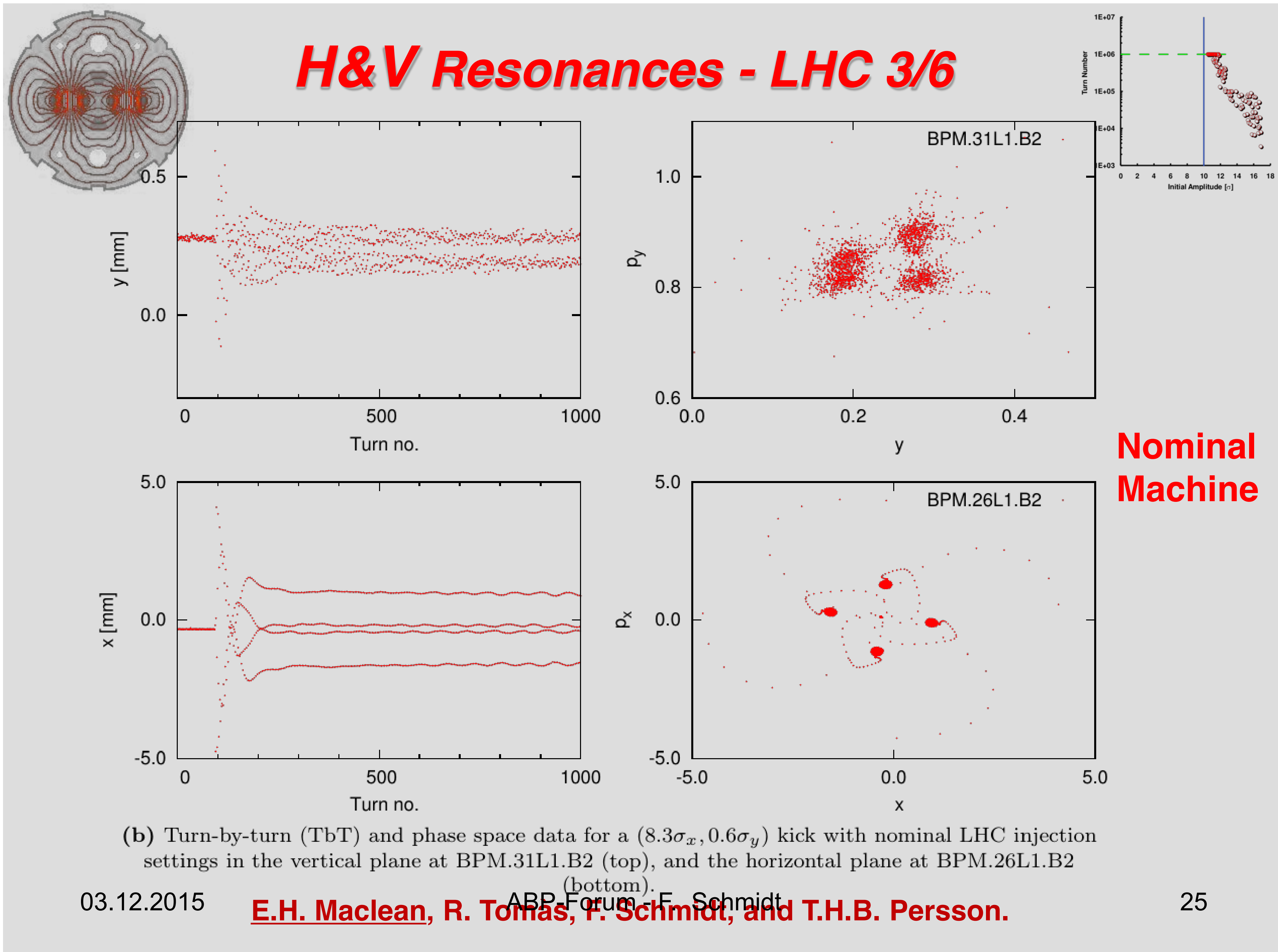

LHC Dynamic Aperture Measurements

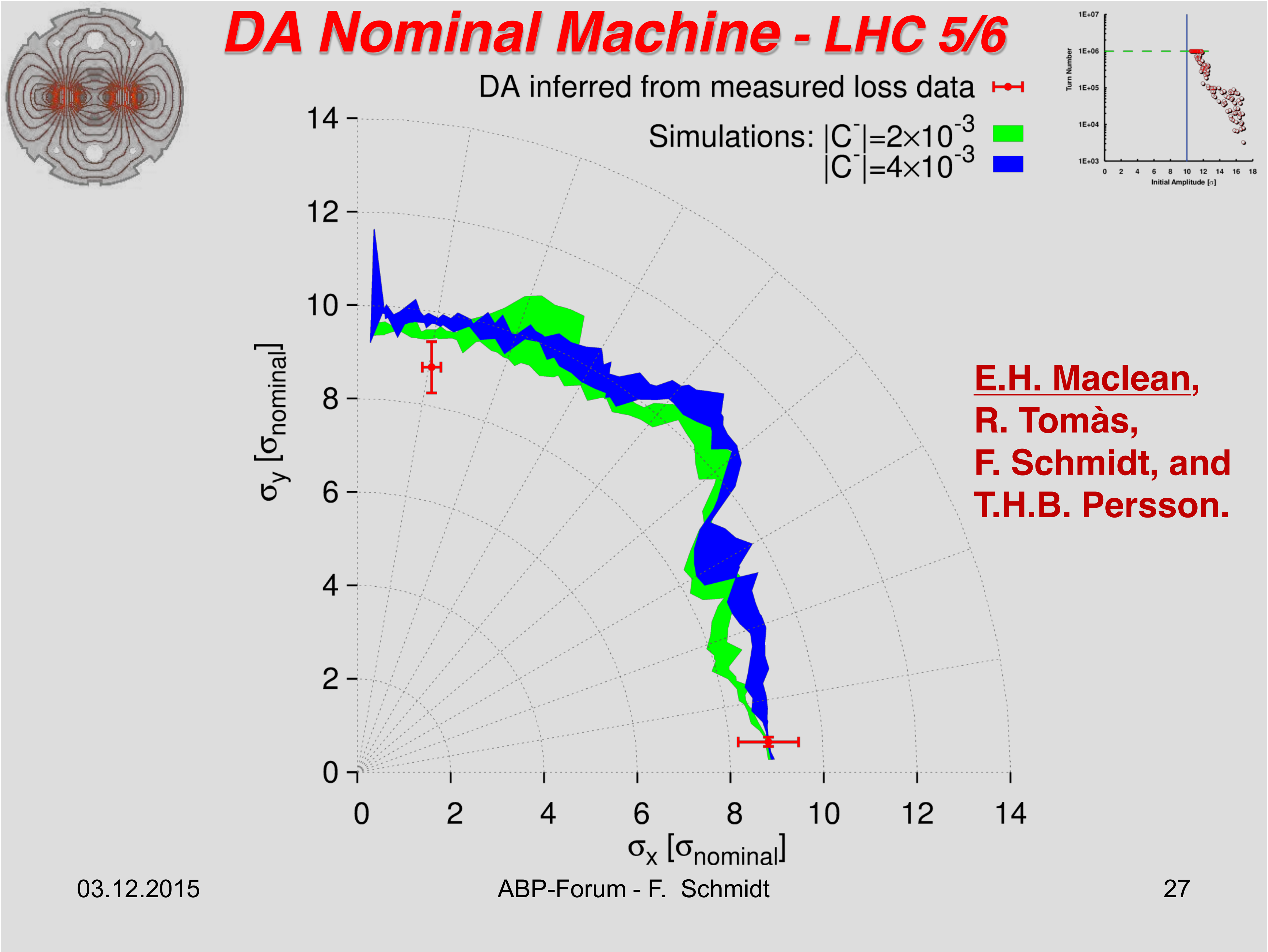

LHC Dynamic Aperture Measurements

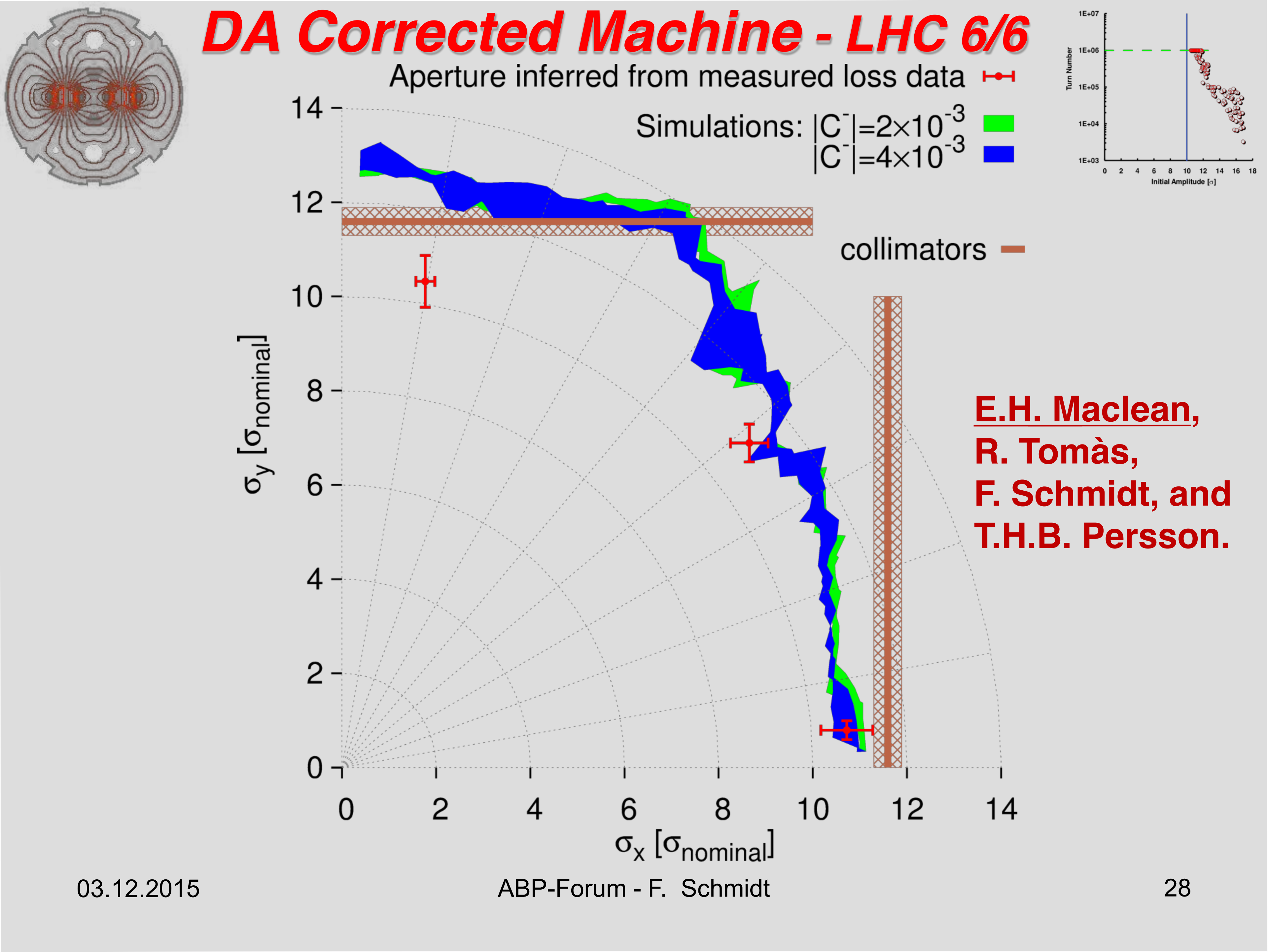

Diffusion Measurements

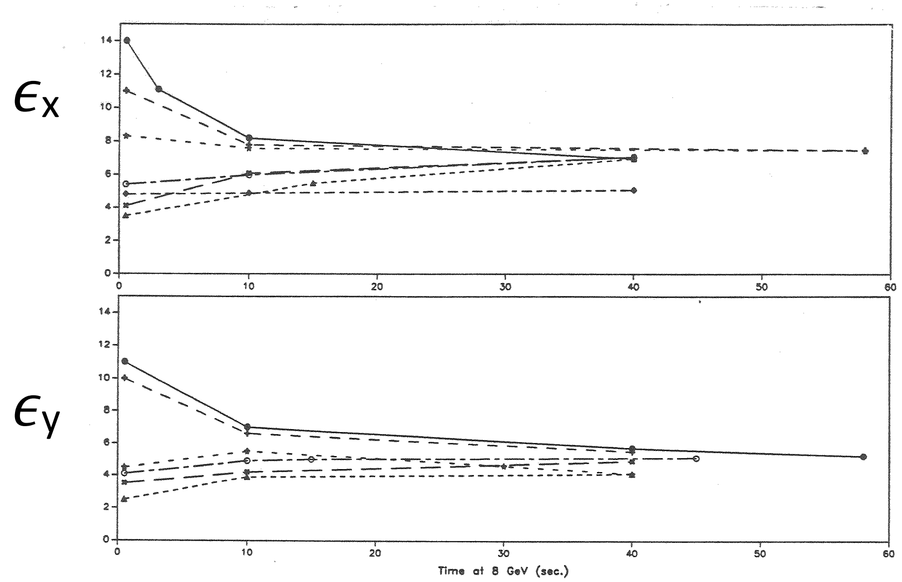

Figure 1: Emittance versus time for beam with different injected emittances.

Main Ring measurements *circa* 1988

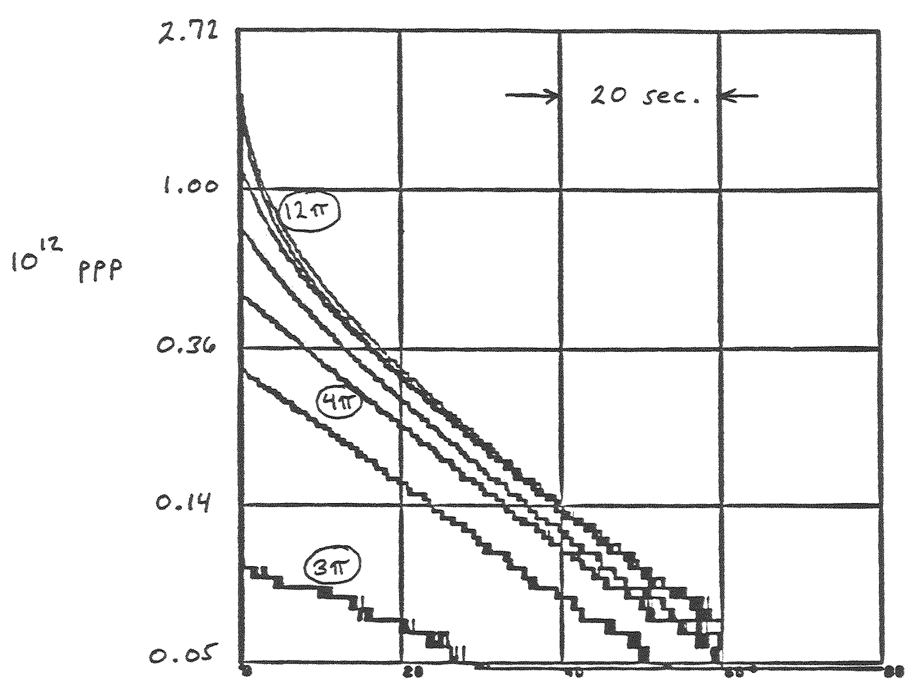

Tevatron Measurements, *circa* 2007

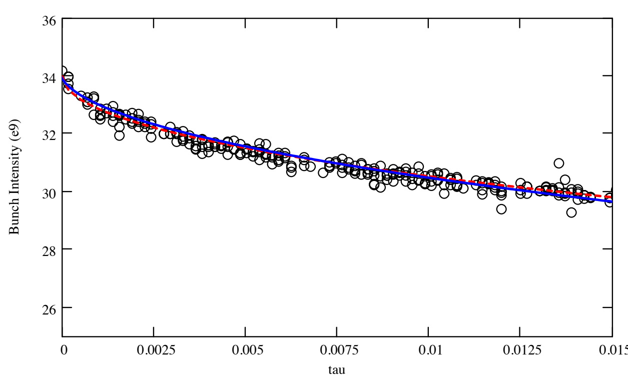

Figure 15: **Plot of antiproton intensity data versus τ for Collider Store 1886. Here, $t/\tau = W/R \approx 5.5$ hr. Two curves are present also: $N(\tau)$ (solid) and $N_0 \exp(-\sqrt{\tau})$ (dashed) for an initial uniform distribution out to the admittance.**

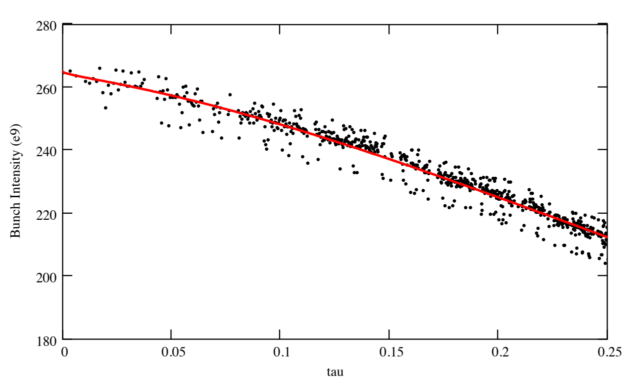

Figure 16: **Plot of proton intensity data versus τ for Collider Store 1971 along with the curve $N(\tau)$ for an initial distribution which is Gaussian out to an aperture at $a = 3\sigma_0$. Here, $t/\tau = W/R \approx 2$ hr.**